

PARTIAL RELINQUISHMENT REPORT

Ringwood EL32244

Titleholder : Gempart (NT) Pty Ltd

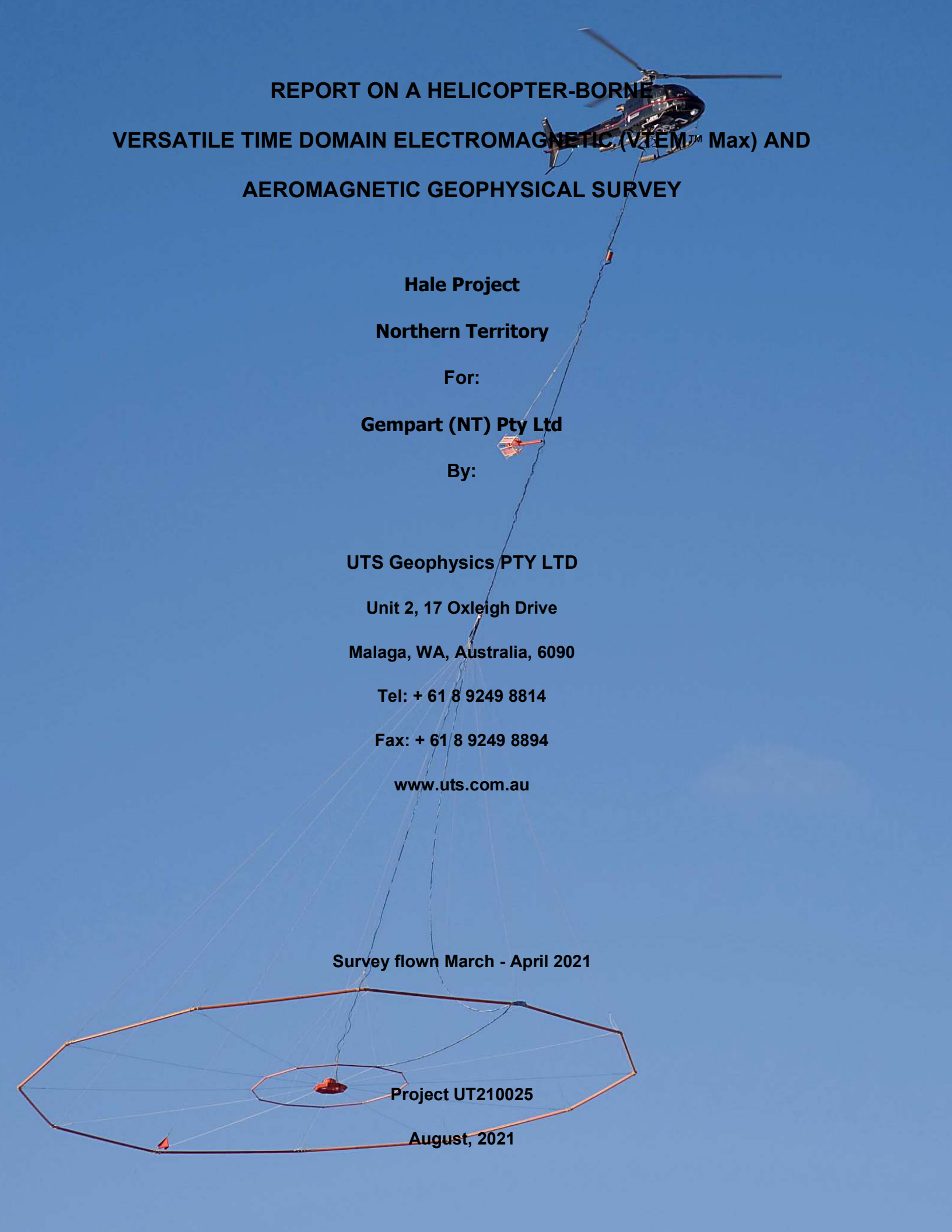
EXPLORATION LICENCE EL32244

FOR THE PERIOD 20/03/2020 to 19/03/2022

APPENDIX 2

VTEM SURVEY LOGISTICS REPORT

Pages with content not relevant to EL32244 have been edited out.



**REPORT ON A HELICOPTER-BORNE
VERSATILE TIME DOMAIN ELECTROMAGNETIC (VTEM™ Max) AND
AEROMAGNETIC GEOPHYSICAL SURVEY**

Hale Project

Northern Territory

For:

Gempart (NT) Pty Ltd

By:

UTS Geophysics PTY LTD

Unit 2, 17 Oxleigh Drive

Malaga, WA, Australia, 6090

Tel: + 61 8 9249 8814

Fax: + 61 8 9249 8894

www.uts.com.au

Survey flown March - April 2021

Project UT210025

August, 2021

TABLE OF CONTENTS

1. INTRODUCTION.....	1
1.1 General Considerations	1
1.2 Survey and System Specifications.....	2
1.3 Topographic Relief and Cultural Features.....	3
2. DATA ACQUISITION.....	6
2.1 Survey Area	6
2.2 Survey Operations.....	6
2.3 Flight Specifications.....	7
2.4 Aircraft and Equipment	7
2.4.1 Survey Aircraft.....	7
2.4.2 Electromagnetic System	7
2.4.3 Airborne magnetometer	11
2.4.4 Full Waveform VTEM™ Sensor Calibration.....	11
2.4.5 Radar Altimeter.....	12
2.4.6 GPS Navigation System	12
2.4.7 Digital Acquisition System.....	12
2.5 Base Station.....	12
3. PERSONNEL.....	13
4. DATA PROCESSING AND PRESENTATION	14
4.1 Flight Path.....	14
4.2 Electromagnetic Data.....	14
4.3 Magnetic Data	16
4.4 TAU Parameter and CVG Calculation.....	16
5. DELIVERABLES	17
5.1 Survey Report	17
5.2 Maps.....	17
5.3 Digital Data	18
6. CONCLUSIONS AND RECOMMENDATIONS	22

LIST OF FIGURES

Figure 1: Property Location.....	1
Figure 2: Survey area location on Google Earth.	2
Figure 3: Flight path over a Google Earth Image – Arumbera (A1).....	3
Figure 4: Flight path over a Google Earth Image – South Numery (A2).....	4
Figure 5: Flight path over a Google Earth Image – Ringwood (A3).....	4
Figure 6: Flight path over a Google Earth Image – No.5 Bore (A4).....	5
Figure 7: Flight path over a Google Earth Image – Kay Creek (A5)	5
Figure 8: VTEM™ Waveform.....	8
Figure 9: VTEM™ Max System Configuration.	11
Figure 10: Z, X and Fraser filtered X (FFx) components for “thin” target.	15

LIST OF TABLES

Table 1: Survey Specifications	6
Table 2: Survey schedule	6
Table 3: Off-Time Decay Sampling Scheme	8
Table 4: Acquisition Sampling Rates	12
Table 5: Geosoft GDB Data Format	18
Table 6: Geosoft Resistivity Depth Image GDB Data Format.....	20
Table 7: Geosoft Waveform GDB Data Format.....	20

APPENDICES

A. Survey location maps	A1
B. Survey Block Coordinates	B1
C. Geophysical Maps	C1
D. Generalized Modelling Results of the VTEM System.....	D1
E. EM Time Constant (TAU) Analysis	E1
F. TEM Resistivity Depth Imaging (RDI)	F1
G. Resistivity Depth Images (RDI)	G1

EXECUTIVE SUMMARY

HALE PROJECT EAST OF ALICE SPRINGS, NORTHERN TERRITORY

During March 22nd to April 13th, 2021, 2021 UTS Geophysics Pty Ltd carried out a helicopter-borne geophysical survey over the Hale Project area, east of Alice Springs, Northern Territory.

Principal geophysical sensors included a versatile time domain electromagnetic (VTEM™ Max) system, and a cesium magnetometer. Ancillary equipment included a GPS navigation system and a radar altimeter. A total of 2019 line-kilometres of geophysical data were acquired during the survey.

In-field data quality assurance and preliminary processing were carried out on a daily basis during the acquisition phase. Preliminary and final data processing, including generation of final digital data and map products were undertaken from the office of UTS Geophysics in Aurora, Ontario.

The processed survey results are presented as the following maps:

- Electromagnetic stacked profiles of the B-field Z Components,
- Electromagnetic stacked profiles of dB/dt Z Components,
- B-Field Z Component Channel grid,
- dB/dt Z Component Channel grid,
- Fraser Filtered dB/dt X Component Channel grid,
- Reduced to Pole (RTP) Total Magnetic Intensity (TMI),
- Calculated Vertical Gradient, Reduced to Pole (RTP_CVG);
- Calculated Time Constant (Tau) with RTP_CVG contours,
- Resistivity Depth Imaging (RDI) sections and depth-slices are presented.

Digital data includes all electromagnetic and magnetic products, plus ancillary data including the waveform.

The survey report describes the procedures for data acquisition, description of equipment, processing, final image presentation and the specifications for the digital data set.

1. INTRODUCTION

1.1 General Considerations

UTS Geophysics Pty Ltd performed a helicopter-borne geophysical survey over Hale Project in Northern Territory (Figure 1).

Alistair Mackie and Graham Bubner represented Gempart (NT) Pty Ltd during the data acquisition and data processing phases of this project.

The geophysical surveys consisted of helicopter borne EM using the versatile time-domain electromagnetic (VTEM™) Max system with Full-Waveform processing. Measurements consisted of Vertical (Z) and In-line Horizontal (X & Y) components of the EM fields using an induction coil and the aeromagnetic total field using a cesium magnetometer. A total of 2019 line-km of geophysical data were acquired during the survey.

The crew was based out of Ross River (Figure 2) in Northern Territory for the acquisition phase of the survey. Survey flying occurred on April 1st to April 12th, 2021.

Data quality control and quality assurance, and preliminary data processing were carried out on a daily basis during the acquisition phase of the project. Final data processing followed immediately after the end of the survey. Final reporting, data presentation and archiving were completed from the Aurora office of UTS Geophysics Pty Ltd. in August 2021.

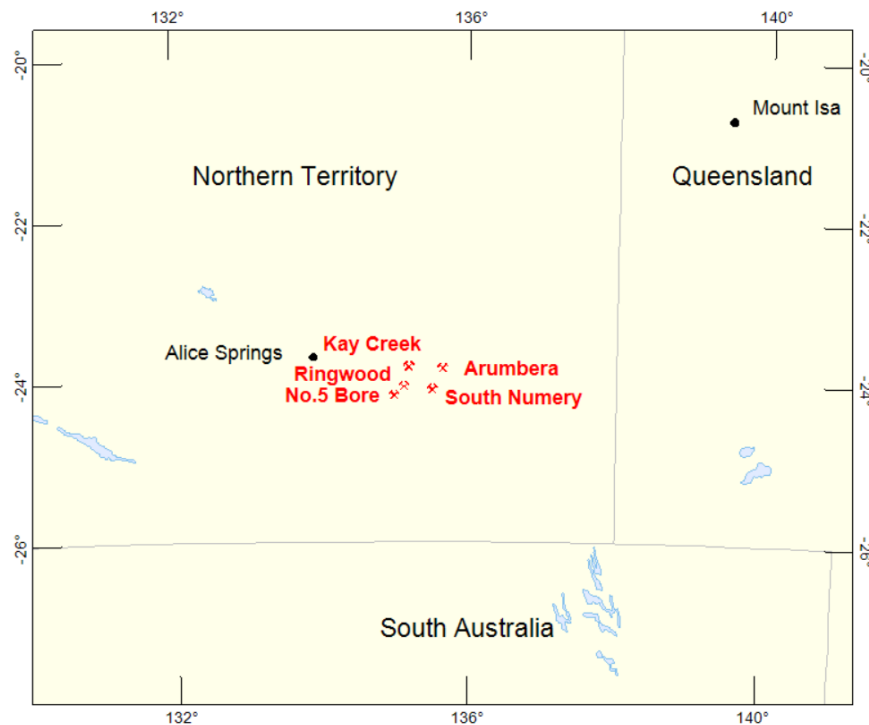


Figure 1: Property Location.

1.2 Survey and System Specifications

Hale Project was carried out over five blocks. All blocks lie approximately 120 to 185 kilometres east of Alice Springs, NT. (see Figure 2 below).

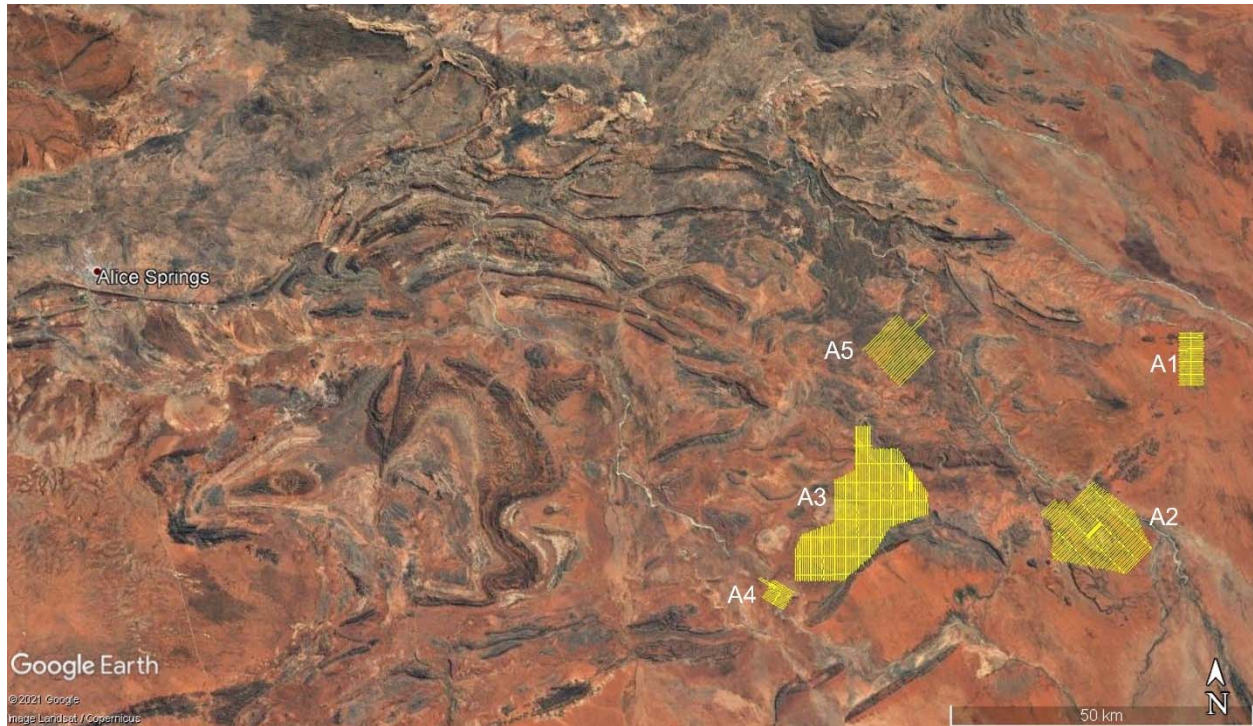


Figure 2: Survey area location on Google Earth.

The Hale Project survey areas were flown in various directions. Arumbera (A1) was flown in a west to east ($N 90^\circ E$ azimuth) direction with traverse line spacing of 300m, as depicted in Figure 3. A single tie line was flown perpendicular to the traverse line. South Numery (A2) was flown in a southwest to northeast ($N 45^\circ E$ azimuth) direction with traverse line spacing of 100-300m, as depicted in Figure 4. Tie lines were flown perpendicular to the traverse line at 3000m line spacings. Ringwood (A3) was flown in a south to north ($N 0^\circ E$ azimuth) direction with traverse line spacing of 100-300m, as depicted in Figure 5. Tie lines were flown perpendicular to the traverse lines at 3000m line spacings. No.5 Bore (A4) was flown in a northwest to southeast ($N 120^\circ E$ azimuth) direction with traverse line spacing of 300m, as depicted in Figure 6. A single tie line was flown perpendicular to the traverse line. Finally, Kay Creek (A5) was flown in a southwest to northeast ($N 45^\circ E$ azimuth) direction with traverse line spacing of 100-300m, as depicted in Figure 7. For more detailed information on the flight spacing and direction, see Table 1.

1.3 Topographic Relief and Cultural Features

Topographically, the survey areas exhibit relief with elevations ranging from 272 to 545 metres above mean sea level, over a total area of 575 square kilometres (Figure 3 - 7).

There are no signs of culture throughout the Hale Project survey areas.

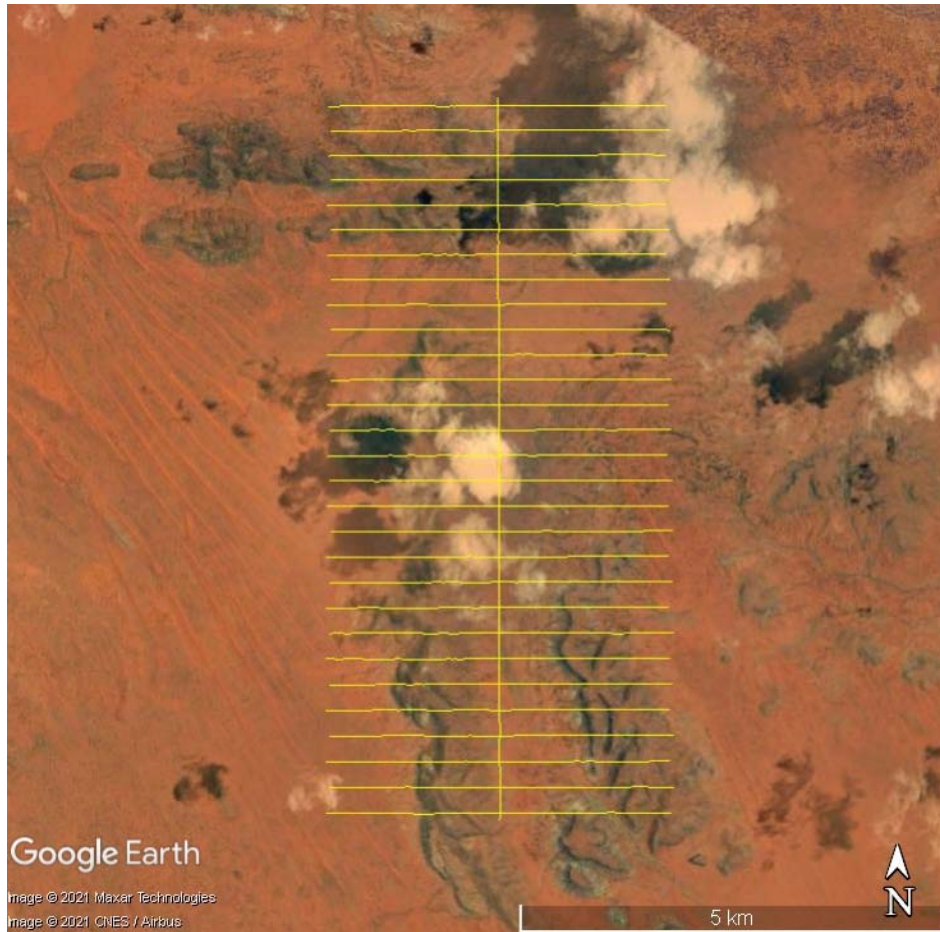


Figure 3: Flight path over a Google Earth Image – Arumbera (A1)

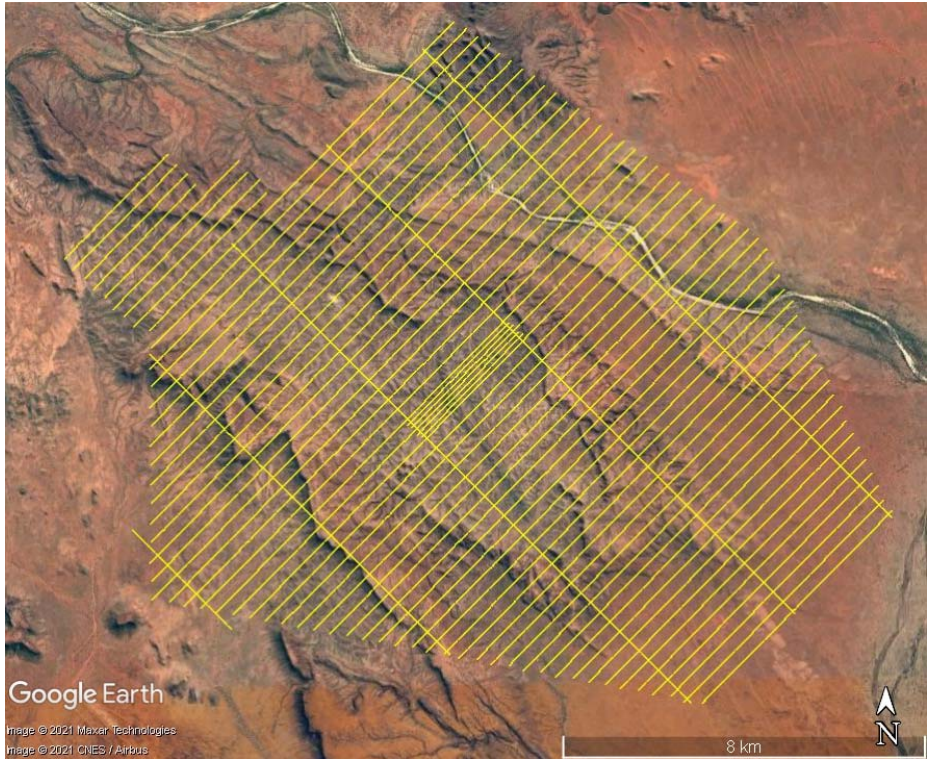


Figure 4: Flight path over a Google Earth Image – South Numery (A2)

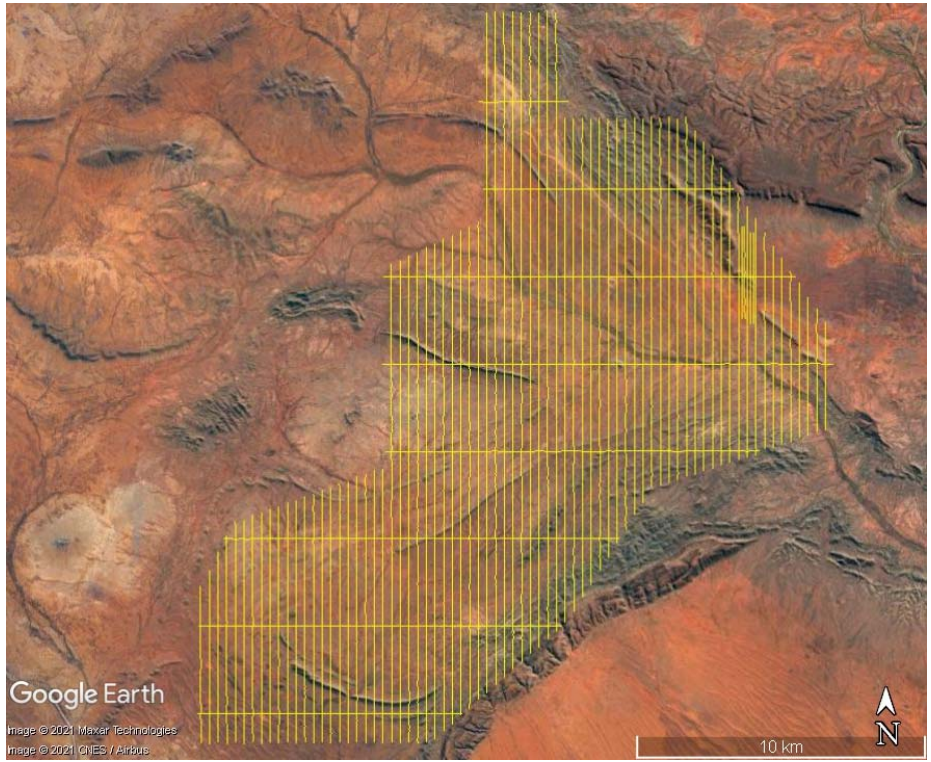


Figure 5: Flight path over a Google Earth Image – Ringwood (A3)

2. DATA ACQUISITION

2.1 Survey Area

The survey block (see Figure 3 - 7 and Appendix A) and general flight specifications are as follows:

Table 1: Survey Specifications

Survey block	Line spacing (m)	Area (Km ²)	Planned ¹ Line-km	Actual Line-km	Flight direction	Line numbers
Arumbera (A1)	Traverse: 300	37	125	127	N90°E / N270°E	L1000 – L1280
	Tie Lines: N/A				N0°E / N180°E	T2000
South Numery (A2)	Traverse: 300	174	594	641	N45°E / N225°E	L2200 – L3480
	Tie Lines: 3000				N135°E / N315°E	T4000 – T4040
Ringwood (A3)	Traverse: 300	273	980	1006	N0°E / N180°E	L5000 – L5720
	Tie Lines: 3000				N90°E / N270°E	T6000 – T6070
No.5 Bore (A4)	Traverse: 300	16	51	59	N120°E / N300°E	L7000 – L7110
	Tie Lines: N/A				N30°E / N210°E	T8000
Kay Creek (A5)	Traverse: 300	75	184	186	N45°E / N225°E	L9000 – L9210
	Tie Lines: N/A				N/A	N/A
TOTAL		575	1934	2019		

Survey block boundaries co-ordinates are provided in Appendix B.

2.2 Survey Operations

Survey operations were based out of Ross River, NT from March 26th to April 13th, 2021. The following table shows the timing of the flying.

Table 2: Survey schedule

Date	Comments
22-Mar-21	Mobilization to Port Augusta, SA
23-Mar-21	Mobilization to Coober Pedy, SA
24-Mar-21	Mobilization to Alice Springs, NT
25-Mar-21	Mobilization to Ross River, local logistics
26-Mar-21	System assembly
27-Mar-21	System assembly, local logistics
28-Mar-21	System assembly, set up base mag
29-Mar-21	Reconnaissance and test flights
30-Mar-21	Local logistics

¹ Note: Actual Line kilometres represent the total line kilometres in the final database. These line-km normally exceed the Planned Line-km, as indicated in the survey NAV files.

Date	Comments
31-Mar-21	Local logistics
01-Apr-21	Production Flights - 207.3 km flown
02-Apr-21	Helicopter repairs
03-Apr-21	Helicopter repairs
04-Apr-21	Production Flights - 306.3 km flown
05-Apr-21	Production Flights - 333.8 km flown
06-Apr-21	Production Flights - 184.2 km flown
07-Apr-21	Production Flights - 184 km flown
08-Apr-21	Production Flights - 313.5 km flown
09-Apr-21	Production Flights - 280.7 km flown
10-Apr-21	Production Flights - 124.6 km flown
11-Apr-21	Standby for infill lines
12-Apr-21	Production Flights - 58.5 km flown
13-Apr-21	Demobilization

2.3 Flight Specifications

Over all five survey areas, the helicopter was maintained at a mean altitude of 82 metres above the ground with an average survey speed of 87 km/hour. This allowed for an actual average transmitter-receiver loop terrain clearance of 34 metres and a magnetic sensor clearance of 72 metres.

The on-board operator was responsible for monitoring the system integrity. He also maintained a detailed flight log during the survey, tracking the times of the flight as well as any unusual geophysical or topographic features.

On return of the aircrew to the base camp the survey data was transferred from a compact flash card (PCMCIA) to the data processing computer. The data were then uploaded via ftp to the UTS office in Aurora for daily quality assurance and quality control by qualified personnel.

2.4 Aircraft and Equipment

2.4.1 Survey Aircraft

The survey was flown using a Eurocopter AS 350 B3 helicopter, registration VH-VIM. The helicopter is owned and operated by United Aero Helicopters. Installation of the geophysical and ancillary equipment was carried out by a UTS Geophysics Pty Ltd crew.

2.4.2 Electromagnetic System

The electromagnetic system was a UTS Time Domain EM (VTEM™ Max) full receiver-waveform streamed data recorded system. The “full waveform VTEM™ system” uses the streamed half-cycle recording of transmitter and receiver waveforms to obtain a complete system response calibration throughout the entire survey flight. VTEM™, with the serial number 24 had been used for the survey. The configuration is as indicated in Figure 9.

The VTEM™ Max Receiver and transmitter coils were in concentric-coplanar and Z-direction oriented configuration. The receiver system for the project also included coincident-coaxial X- and Y-direction coils to measure the in-line dB/dt and calculate B-Field responses. The EM transmitter-receiver loop was towed at a mean distance of 48 metres below the aircraft as shown in Figure 9. The receiver decay recording scheme is shown in Figure 8.

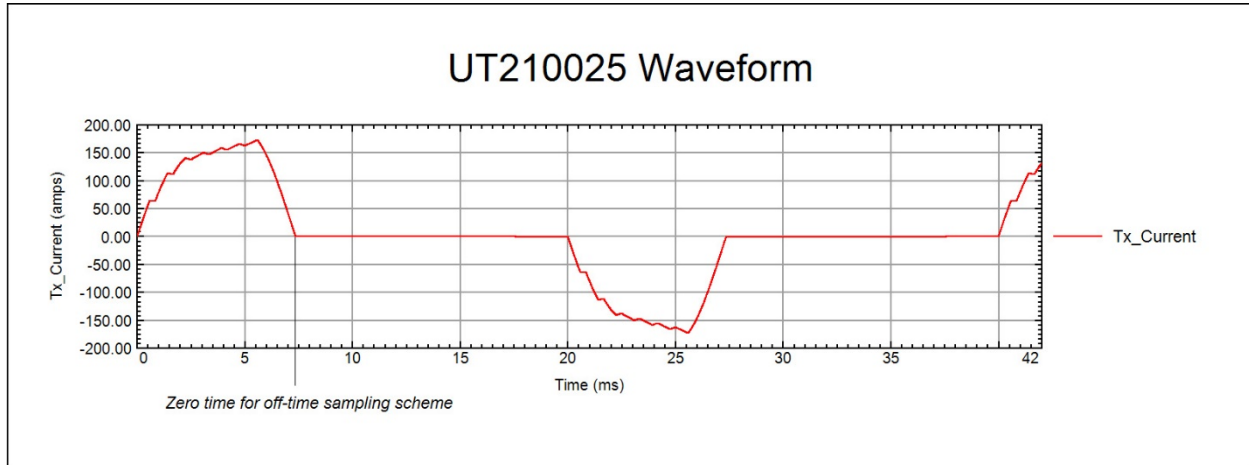


Figure 8: VTEM™ Waveform

The VTEM™ decay sampling scheme is shown in Table 3 below. Forty five time measurement gates were used for the final data processing in the range from 0.021 to 10.667 msec. Zero time for off-time sampling scheme is equal to current pulse width and defined as the time near the end of the turn-off ramp where the dl/dt waveform falls to 1/2 of its peak value.

Table 3: Off-Time Decay Sampling Scheme

VTEM™ Decay Sampling Scheme				
index	Start	End	Middle	Window
Milliseconds				
4	0.018	0.023	0.021	0.005
5	0.023	0.029	0.026	0.005
6	0.029	0.034	0.031	0.005
7	0.034	0.039	0.036	0.005
8	0.039	0.045	0.042	0.006
9	0.045	0.051	0.048	0.007
10	0.051	0.059	0.055	0.008
11	0.059	0.068	0.063	0.009
12	0.068	0.078	0.073	0.010
13	0.078	0.090	0.083	0.012
14	0.090	0.103	0.096	0.013
15	0.103	0.118	0.110	0.015
16	0.118	0.136	0.126	0.018

VTEM™ Decay Sampling Scheme				
index	Start	End	Middle	Window
Milliseconds				
17	0.136	0.156	0.145	0.020
18	0.156	0.179	0.167	0.023
19	0.179	0.206	0.192	0.027
20	0.206	0.236	0.220	0.030
21	0.236	0.271	0.253	0.035
22	0.271	0.312	0.290	0.040
23	0.312	0.358	0.333	0.046
24	0.358	0.411	0.383	0.053
25	0.411	0.472	0.440	0.061
26	0.472	0.543	0.505	0.070
27	0.543	0.623	0.580	0.081
28	0.623	0.716	0.667	0.093
29	0.716	0.823	0.766	0.107
30	0.823	0.945	0.880	0.122
31	0.945	1.086	1.010	0.141
32	1.086	1.247	1.161	0.161
33	1.247	1.432	1.333	0.185
34	1.432	1.646	1.531	0.214
35	1.646	1.891	1.760	0.245
36	1.891	2.172	2.021	0.281
37	2.172	2.495	2.323	0.323
38	2.495	2.865	2.667	0.370
39	2.865	3.292	3.063	0.427
40	3.292	3.781	3.521	0.490
41	3.781	4.341	4.042	0.560
42	4.341	4.987	4.641	0.646
43	4.987	5.729	5.333	0.742
44	5.729	6.581	6.125	0.852
45	6.581	7.560	7.036	0.979
46	7.560	8.685	8.083	1.125
47	8.685	9.977	9.286	1.292
48	9.977	11.458	10.667	1.482

Z Component: 04-48 time gates

X Component: 20-48 time gates

Y Component: 20-48 time gates

VTEM™ Max system specification:

Transmitter

- Transmitter loop diameter: 35 m
- Effective Transmitter loop area: 3848.45 m²
- Number of turns: 4
- Transmitter base frequency: 25 Hz
- Peak current: 177.0 A
- Pulse width: 7.35 ms
- Wave form shape: trapezoid
- Peak dipole moment: 681175.25 nIA
- Average transmitter-receiver loop terrain clearance: 34 metres

Receiver

X Coil diameter: 0.32 m

- Number of turns: 245
- Effective coil area: 19.69 m²

Y Coil diameter: 0.32 m

- Number of turns: 245
- Effective coil area: 19.69 m²

Z-Coil diameter: 1.2 m

- Number of turns: 100
- Effective coil area: 113.04 m²

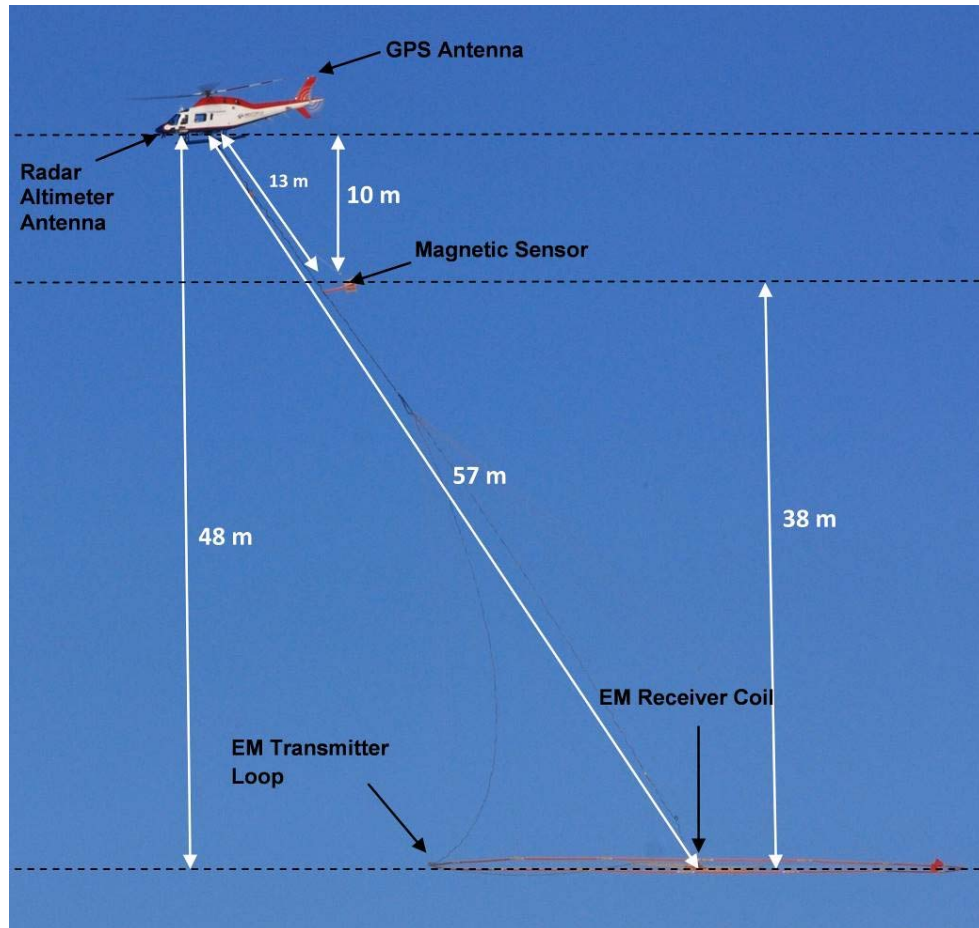


Figure 9: VTEM™ Max System Configuration.

2.4.3 Airborne magnetometer

The magnetic sensor utilized for the survey was Geometrics optically pumped cesium vapour magnetic field sensor mounted 10 metres below the helicopter, as shown in Figure 9. The sensitivity of the magnetic sensor is 0.02 nanoTesla (nT) at a sampling interval of 0.1 seconds.

2.4.4 Full Waveform VTEM™ Sensor Calibration

The calibration is performed on the complete VTEM™ system installed in and connected to the helicopter, using special calibration equipment. This calibration takes place on the ground at the start of the project prior to surveying.

The procedure takes half-cycle files acquired and calculates a calibration file consisting of a single stacked half-cycle waveform. The purpose of the stacking is to attenuate natural and man-made magnetic signals, leaving only the response to the calibration signal.

This calibration allows the transfer function between the EM receiver and data acquisition system and also the transfer function of the current monitor and data acquisition system to be determined. These calibration results are then used in VTEM™ full waveform processing.

2.4.5 Radar Altimeter

A Terra TRA 3000/TRI 40 radar altimeter was used to record terrain clearance. The antenna was mounted beneath the bubble of the helicopter cockpit (Figure 9).

2.4.6 GPS Navigation System

The navigation system used was a UTS PC104 based navigation system utilizing a NovAtel's WAAS (Wide Area Augmentation System) enabled GPS receiver, UTS navigate software, a full screen display with controls in front of the pilot to direct the flight and a NovAtel GPS antenna mounted on the helicopter tail (Figure 9). As many as 11 GPS and two WAAS satellites may be monitored at any one time. The positional accuracy or circular error probability (CEP) is 1.8 m, with WAAS active, it is 1.0 m. The co-ordinates of the block were set-up prior to the survey and the information was fed into the airborne navigation system.

2.4.7 Digital Acquisition System

A UTS data acquisition system recorded the digital survey data on an internal compact flash card. Data is displayed on an LCD screen as traces to allow the operator to monitor the integrity of the system. The data type and sampling interval as provided in Table 4.

Table 4: Acquisition Sampling Rates

Data Type	Sampling
TDEM	0.1 sec
Magnetometer	0.1 sec
GPS Position	0.1 sec
Radar Altimeter	0.2 sec

2.5 Base Station

A combined magnetometer/GPS base station was utilized on this project. A Geometrics Cesium vapour magnetometer was used as a magnetic sensor with a sensitivity of 0.001 nT. The base station was recording the magnetic field together with the GPS time at 1 Hz on a base station computer.

The base station magnetometer sensor was set away from electric transmission lines and moving ferrous objects such as motor vehicles. The base station data were backed-up to the data processing computer at the end of each survey day.

3. PERSONNEL

The following UTS Ltd. personnel were involved in the project.

Field:

Project Manager:	Hayley Kelly (Office)
Data QC:	Marta Orta (Office) Gaurav Nailwal (Office)
Crew chief:	Peter MacDonald
Operator:	Adrian Page

The survey pilot and the mechanical engineer were employed directly by the helicopter operator – United Aero Helicopters

Pilot:	Charlie Elliot
Mechanical Engineer:	Contracted third party provider

Office:

Preliminary Data Processing:	Marta Orta Gaurav Nailwal
Final Data Processing:	Andrea Reman
Data QA/QC:	Emily Data Jean Legault
Reporting/Mapping:	Emily Data

Processing and Interpretation phases were carried out under the supervision of Emily Data, and Jean M. Legault, M.Sc.A, P.Eng, and P.Geo - Chief Geophysicist. The customer relations were looked after by Levin Lee.

4. DATA PROCESSING AND PRESENTATION

Data compilation and processing were carried out by the application of Geosoft OASIS Montaj and programs proprietary to UTS Geophysics Ltd.

4.1 Flight Path

The flight path, recorded by the acquisition program as WGS84 latitude/longitude, was converted into WGS 84 UTM Zone 53S coordinate system in Oasis Montaj.

The flight path was drawn using linear interpolation between x, y positions from the navigation system. Positions are updated every second and expressed as UTM easting's (x) and UTM northing's (y).

4.2 Electromagnetic Data

The Full Waveform EM specific data processing operations included:

- Half cycle stacking (performed at time of acquisition);
- System response correction;
- Parasitic and drift removal by deconvolution.

A three-stage digital filtering process was used to reject major spheric events and to reduce system noise. Local spheric activity can produce sharp, large amplitude events that cannot be removed by conventional filtering procedures. Smoothing or stacking will reduce their amplitude but leave a broader residual response that can be confused with geological phenomena. To avoid this possibility, a computer algorithm searches out and rejects the major spheric events.

The signal to noise ratio was further improved by the application of a low pass linear digital filter. This filter has zero phase shift which prevents any lag or peak displacement from occurring, and it suppresses only variations with a wavelength less than about 1 second or 15 metres. This filter is a symmetrical 1 sec linear filter.

The results are presented as stacked profiles of EM voltages for the time gates, in linear - logarithmic scale for the B-field Z component and dB/dt responses in the Z, and X components. B-field Z component time channel recorded at 0.880 milliseconds after the termination of the impulse is also presented as contour colour images. Fraser Filter X component is also presented as a colour image. Calculated Time Constant (TAU) with Calculated Vertical Derivative RTP contours is presented in Appendix C and E. Resistivity Depth Image (RDI) is also presented in Appendix F and G.

VTEM™ Max has three receiver coil orientations. Z-axis coil is oriented parallel to the transmitter coil axis and both are horizontal to the ground. The X-axis coil is oriented parallel to the ground and along the line-of-flight. The Y-axis coil is oriented parallel to the ground and perpendicular to the line-of-flight. The combination of the X, Y and Z coils configuration provides information on the position, depth, dip, and thickness of a conductor. Generalized modeling results of VTEM™ Max data are shown in Appendix D.

In general X-component data produce cross-over type anomalies: from “+ to –” in flight direction of flight for “thin” sub vertical targets and from “- to +” in direction of flight for “thick” targets. Z component data produce double peak type anomalies for “thin” sub vertical targets and single peak for “thick” targets.

The limits and change-over of “thin-thick” depends on dimensions of a TEM system.

Because of X component polarity is under line-of-flight, convolution Fraser filter (FF, Figure 10) is applied to X component data to represent axes of conductors in the form of grid map. In this case positive FF anomalies always correspond to “plus-to-minus” X data crossovers independently of direction of flight.

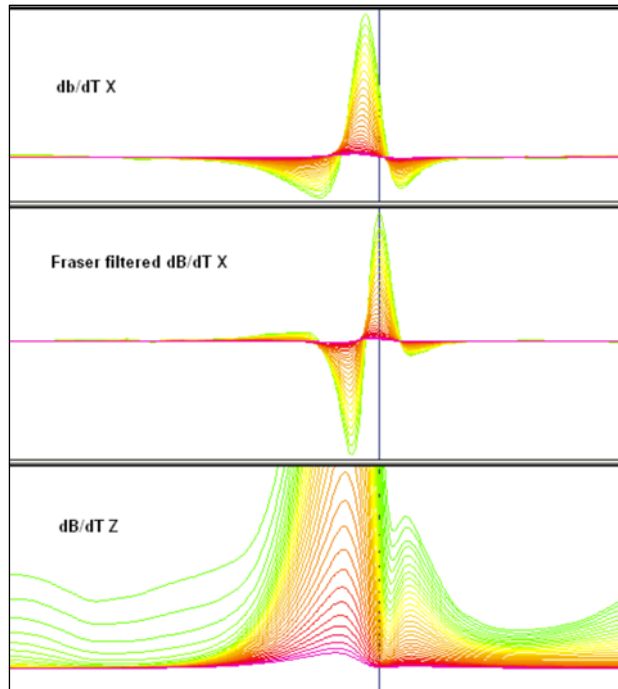


Figure 10: Z, X and Fraser filtered X (FFx) components for “thin” target.

4.3 Magnetic Data

The processing of the magnetic data involved the correction for diurnal variations by using the digitally recorded ground base station magnetic values. The base station magnetometer data was edited and merged into the Geosoft GDB database on a daily basis. The aeromagnetic data was corrected for diurnal variations by subtracting the observed magnetic base station deviations.

The corrected magnetic data was interpolated between survey lines using a random point gridding method to yield x-y grid values for a standard grid cell size of approximately 75 metres at the mapping scale. The Minimum Curvature algorithm was used to interpolate values onto a rectangular regular spaced grid.

4.4 TAU Parameter and CVG Calculation

The processed VTEMTM survey results are presented as a calculated dB/dt Z-component time constant (Tau), which is an indicator of geological unit's electrical conductance.

An explanation of the EM time constant calculation is provided in Appendix F. The TAU dB/dt Z-component map is presented as Figure D-6 in Appendix D and in Appendix C. The TAU grid contour map is accompanied by an overlay of the calculated vertical gradient of RTP_TMI anomaly contours for tracing possible EM-MAG anomaly correlations.

The calculated vertical magnetic gradient (RTP_CVG) contour layer, on the top of TAU color grid, generally is more representative of the smaller scale and shallower magnetic sources in comparison with the TMI. CVG is designed to emphasize the structures and lithological units that might not otherwise be seen on the RTP_TMI due to the nearby presence of stronger magnetic responses, showing a high resolution in terms of individual structures.

As can be seen from the combined TAU-RTP_CVG map, the most highly conductive targets (with maximal TAU) are very strongly correlated with sources of magnetic anomalies.

5. DELIVERABLES

5.1 Survey Report

The survey report describes the data acquisition, processing, and final presentation of the survey results. The survey report is provided in two paper copies and digitally in PDF format.

5.2 Maps

Final maps were produced at various scales to allow for best representation of the survey size and line spacing. The coordinate/projection system used was GDA 94 Datum, MGA Zone 53. All maps show the flight path trace and topographic data; latitude and longitude are also noted on maps.

The final results of the survey are presented as EM profiles, a late-time gate gridded EM channel, and a colour magnetic TMI contour map.

- Maps at various scales in Geosoft MAP format, as follows:

UT210025_**_dBdt:	dB/dt profiles Z Component, Time Gates 0.220 – 7.036 ms in linear – logarithmic scale.
UT210025_**_BField:	B-field profiles Z Component, Time Gates 0.220 – 7.036 ms in linear – logarithmic scale over RTP
UT210025_**_CVG_RTP:	Calculated Vertical Gradient (CVG) of Reduced to Pole (RTP) Total Magnetic Intensity
UT210025_**_BFz30:	B-field late time Z Component Channel 30, Time Gate 0.880 ms
UT210025_**_RTP:	Total Magnetic Intensity Reduced to Pole
UT210025_**_SFxFF30:	Fraser Filtered dB/dt X Component, Channel 30, Time Gate 0.880 ms
UT210025_**_SFz30:	dB/dt Z Component Channel 30, Time Gate 0.880 ms
UT210025_**_TauSF:	dB/dt Calculated Z-Component Time Constant (Tau) with Calculated Vertical Derivative of RTP contours

Where ** represents block number, block name, and map scale. e.g.,

UT210025_A1_Arumbera_25k_Bfield.map

- Maps are also presented in PDF format.
- Topographic data base was derived from Geoscience Australia 1:250,000 scale (www.ga.gov.au)
- Google Earth files *UT210025_**.kmz* showing the flight path of all 5 blocks is included. ** represents block number and block name. Free versions of Google Earth software from: <http://earth.google.com/download-earth.html>

5.3 Digital Data

- Two copies of the data and maps on DVD were prepared to accompany the report. Each DVD contains a digital file of the line data in GDB Geosoft Montaj format as well as the maps in Geosoft Montaj Map and PDF format.

DVD structure:

Data contains databases, grids, and maps, as described below.
 Report contains a copy of the report and appendices in PDF format.

Databases in Geosoft GDB format, containing the channels listed in Table 5.

Table 5: Geosoft GDB Data Format

Channel name	Units	Description
X	metres	WGS 84 Easting - UTM Zone 53S
Y	metres	WGS 84 Northing - UTM Zone 53S
Longitude	Decimal Degrees	WGS 84 Longitude data
Latitude	Decimal Degrees	WGS 84 Latitude data
Z	metres	GPS antenna elevation (above Geoid)
Zb	metres	EM bird elevation (above Geoid)
Radar	metres	helicopter terrain clearance from radar altimeter
Radarb	metres	Calculated EM transmitter-receiver loop terrain clearance from radar altimeter
DEM	metres	Digital Elevation Model
Gtime	Seconds of the day	GPS time
Mag1	nT	Raw Total Magnetic field data
Basemag	nT	Magnetic diurnal variation data
Mag2	nT	Diurnal corrected Total Magnetic field data
Mag3	nT	Levelled Total Magnetic field data
CVG	nT/m	Calculated Vertical Derivative of Total Magnetic Intensity (TMI)
RTP	nT	Reduced to Pole (RTP) TMI
CVG RTP	nT/m	Calculated Vertical Derivative of RTP TMI
SFz[4]	pV/(A*m ⁴)	Z dB/dt 0.021 millisecond time channel
SFz[5]	pV/(A*m ⁴)	Z dB/dt 0.026 millisecond time channel
SFz[6]	pV/(A*m ⁴)	Z dB/dt 0.031 millisecond time channel
SFz[7]	pV/(A*m ⁴)	Z dB/dt 0.036 millisecond time channel
SFz[8]	pV/(A*m ⁴)	Z dB/dt 0.042 millisecond time channel
SFz[9]	pV/(A*m ⁴)	Z dB/dt 0.048 millisecond time channel
SFz[10]	pV/(A*m ⁴)	Z dB/dt 0.055 millisecond time channel
SFz[11]	pV/(A*m ⁴)	Z dB/dt 0.063 millisecond time channel
SFz[12]	pV/(A*m ⁴)	Z dB/dt 0.073 millisecond time channel
SFz[13]	pV/(A*m ⁴)	Z dB/dt 0.083 millisecond time channel
SFz[14]	pV/(A*m ⁴)	Z dB/dt 0.096 millisecond time channel
SFz[15]	pV/(A*m ⁴)	Z dB/dt 0.110 millisecond time channel
SFz[16]	pV/(A*m ⁴)	Z dB/dt 0.126 millisecond time channel
SFz[17]	pV/(A*m ⁴)	Z dB/dt 0.145 millisecond time channel
SFz[18]	pV/(A*m ⁴)	Z dB/dt 0.167 millisecond time channel
SFz[19]	pV/(A*m ⁴)	Z dB/dt 0.192 millisecond time channel
SFz[20]	pV/(A*m ⁴)	Z dB/dt 0.220 millisecond time channel

Channel name	Units	Description
SFz[21]	pV/(A*m ⁴)	Z dB/dt 0.253 millisecond time channel
SFz[22]	pV/(A*m ⁴)	Z dB/dt 0.290 millisecond time channel
SFz[23]	pV/(A*m ⁴)	Z dB/dt 0.333 millisecond time channel
SFz[24]	pV/(A*m ⁴)	Z dB/dt 0.383 millisecond time channel
SFz[25]	pV/(A*m ⁴)	Z dB/dt 0.440 millisecond time channel
SFz[26]	pV/(A*m ⁴)	Z dB/dt 0.505 millisecond time channel
SFz[27]	pV/(A*m ⁴)	Z dB/dt 0.580 millisecond time channel
SFz[28]	pV/(A*m ⁴)	Z dB/dt 0.667 millisecond time channel
SFz[29]	pV/(A*m ⁴)	Z dB/dt 0.766 millisecond time channel
SFz[30]	pV/(A*m ⁴)	Z dB/dt 0.880 millisecond time channel
SFz[31]	pV/(A*m ⁴)	Z dB/dt 1.010 millisecond time channel
SFz[32]	pV/(A*m ⁴)	Z dB/dt 1.161 millisecond time channel
SFz[33]	pV/(A*m ⁴)	Z dB/dt 1.333 millisecond time channel
SFz[34]	pV/(A*m ⁴)	Z dB/dt 1.531 millisecond time channel
SFz[35]	pV/(A*m ⁴)	Z dB/dt 1.760 millisecond time channel
SFz[36]	pV/(A*m ⁴)	Z dB/dt 2.021 millisecond time channel
SFz[37]	pV/(A*m ⁴)	Z dB/dt 2.323 millisecond time channel
SFz[38]	pV/(A*m ⁴)	Z dB/dt 2.667 millisecond time channel
SFz[39]	pV/(A*m ⁴)	Z dB/dt 3.063 millisecond time channel
SFz[40]	pV/(A*m ⁴)	Z dB/dt 3.521 millisecond time channel
SFz[41]	pV/(A*m ⁴)	Z dB/dt 4.042 millisecond time channel
SFz[42]	pV/(A*m ⁴)	Z dB/dt 4.641 millisecond time channel
SFz[43]	pV/(A*m ⁴)	Z dB/dt 5.333 millisecond time channel
SFz[44]	pV/(A*m ⁴)	Z dB/dt 6.125 millisecond time channel
SFz[45]	pV/(A*m ⁴)	Z dB/dt 7.036 millisecond time channel
SFz[46]	pV/(A*m ⁴)	Z dB/dt 8.083 millisecond time channel
SFz[47]	pV/(A*m ⁴)	Z dB/dt 9.286 millisecond time channel
SFz[48]	pV/(A*m ⁴)	Z dB/dt 10.667 millisecond time channel
SFx	pV/(A*m ⁴)	X dB/dt data for time channels 20 to 48
SFy	pV/(A*m ⁴)	Y dB/dt data for time channels 20 to 48
BFz	(pV*ms)/(A*m ⁴)	Z B-Field data for time channels 4 to 48
BFx	(pV*ms)/(A*m ⁴)	X B-Field data for time channels 20 to 48
BFy	(pV*ms)/(A*m ⁴)	Y B-Field data for time channels 20 to 48
SFxFF	pV/(A*m ⁴)	Fraser filtered X dB/dt
NchanBF		Last channel where the algorithm stops calculation, B-Field
TauBF	milliseconds	Time Constant (Tau) calculated from B-field data
NchanSF		Last channel where the algorithm stops calculation, dB/dt
TauSF	milliseconds	Time Constant (Tau) calculated from dB/dt data
PLM		50 Hz power line monitor

Electromagnetic B-field and dB/dt Z component data is found in array channel format between indexes 4 – 48, and X & Y component data from 20 – 48, as described above.

- Database of the Resistivity Depth Images in Geosoft GDB format, containing the following channels:

Table 6: Geosoft Resistivity Depth Image GDB Data Format

Channel name	Units	Description
Xg	metres	WGS 84 Easting - UTM Zone 53S
Yg	metres	WGS 84 Northing - UTM Zone 53S
Dist	metres	Distance from the beginning of the line
Depth	metres	array channel, depth from the surface
Z	metres	array channel, depth from sea level
AppRes	Ohm-m	array channel, Apparent Resistivity
TR	metres	EM system height from sea level
Topo	metres	digital elevation model
Radarb	metres	Calculated EM transmitter-receiver loop terrain clearance from radar altimeter
SF	pV/(A*m ⁴)	array channel, dB/dT
Mag	nT	RTP data
CVG	nT/m	RTP_CVG data
PLM		50Hz Power Line Monitor
DOI	metres	Depth of Investigation: a measure of VTEM depth effectiveness

- Database of the VTEM™ Waveform “UT210025_Waveform.gdb” in Geosoft GDB format, containing the following channels:

Table 7: Geosoft Waveform GDB Data Format

Channel name	Units	Description
Time	ms	Sampling rate interval, 5.2083 microseconds
Tx_Current	Amp	Output current of the transmitter

- Geosoft Resistivity Depth Image Products:

Sections: Apparent resistivity sections along each line in .GRD and .PDF format

Slices: Apparent resistivity slices at selected depths from 25m to depth of investigation, at an increment of 25m in .GRD and .PDF format

Voxel: 3D Voxel imaging of apparent resistivity data clipped by digital elevation and depth of investigation

- Grids in Geosoft GRD, GeoTIFF format, as follows:

**_DEM:	Digital Elevation Model (metres)
**_RTP_CVG:	Calculated Vertical Derivative of RTP TMI (nT/m)
**_CVG:	Calculated Vertical Derivative of Mag3 (nT/m)
**_RTP:	Total Magnetic Intensity (nT) Reduced to Pole
**_Mag3:	Total Magnetic Intensity (nT)
**_BFz30:	B-Field Z Component Channel 30 (Time Gate 0.880 ms)
**_SFxFF30:	Fraser Filter X Component dB/dt Channel 30 (Time Gate 0.880 ms)
**_SFz15:	dB/dt Z Component Channel 15 (Time Gate 0.110 ms)
**_SFz30:	dB/dt Z Component Channel 30 (Time Gate 0.880 ms)
**_SFz45:	dB/dt Z Component Channel 45 (Time Gate 7.036 ms)
**_TauBF:	B-Field Z-Component Calculated Time Constant (ms)
**_TauSF:	dB/dt Z-Component Calculated Time Constant (ms)
**_PLM:	50Hz power line monitor

Where ** denotes project and block number. e.g., *UT210025_A1_BFz30.grd*

A Geosoft .GRD file has a .GI metadata file associated with it, containing grid projection information. A grid cell size of 75 metres was used.

6. CONCLUSIONS AND RECOMMENDATIONS

A helicopter-borne versatile time domain electromagnetic (VTEMTMMax) geophysical survey has been completed over Hale Project, situated east of Alice Springs, NT, for Gempart (NT) Pty Ltd. The Hale Project consists of five (5) blocks: Arumbera (A1), South Numery (A2), Ringwood (A3), No.5 Bore (A4) and Kay Creek (A5).

The total area coverage is 575 km² and the total survey line coverage is 2019 line kilometres. The principal geophysical sensors included a Full Waveform Time Domain electromagnetic system, and a magnetometer. Results have been presented as stacked profiles, and contoured color images at various scales. A formal Interpretation has not been included in this report, but RDI resistivity-depth imaging was performed in support of the VTEM data.

Based on the geophysical results obtained, a number of anomalous conductive EM and magnetic signatures have been defined. The relationship between the EM and magnetic signatures are highlighted in our TAU dB_Z/dt EM decay time-constant & Calculated Vertical Gradient (CVG) contour maps and the Resistivity-Depth Image (RDI) sections (Appendix C & G).

A1 Arumbera: Magnetically, the Arumbera block shows a general near-constant increase in magnetic intensity from west to east, with a high focused in the southeastern corner. Magnetic CVG contours also suggest shallower minor NS lineament trends throughout the block. Electromagnetically, the block's resistivity distribution is approximately T-shaped, with an east-west resistive unit along the northern border and a 1-1.5km wide NNW-SSE trending higher resistivity band that extends through the center of the remainder of the block. More conductive, north-south trending units flank the resistive band to the east and west, which the westernmost being more anomalously conductive and the easternmost more discontinuous. None of the conductive bodies in this block appear to have a magnetic association and may be related to sedimentary units or possibly saline groundwater. The conductive anomalies in the Arumbera block feature EM dB_Z/dt time constants in the 0.5 to 0.73 ms range, which indicates moderate conductivities. According to RDI imaging results, apparent resistivities of anomalous zones in the Arumbera block are as low as ~3-6 ohm-m and bedrock values reach approx. 1k ohm-m. The estimated depth of the top of the anomalous zones, based on RDI, varies from ~50-100 m and maximum depths of investigation (DOI) vary between approx. 250m->550 m.

A2 South Numery: The South Numery block features a prominent, central, large, NW-SE elongate, intrusion-like magnetic high that extends nearly across the full length of the block. Magnetic CVG derivatives also define other narrow magnetic lineament that flank this magnetic feature, particularly to the southwest. Electromagnetically, the central part of the block where the magnetic anomaly occurs is generally highly resistive, and more conductive, NW-SE trending rocks flank it to the northeast and to the south-east, with a mix of weakly conductive and resistive NW-SE trending rock units in the southwestern part. The northeastern and southeastern conductive units correlate with magnetic lows. The conductive anomalies at South Numery block feature EM dB_Z/dt time constants in the 0.4 to 0.72 ms range, which indicates moderate conductivities. Apparent resistivities of anomalous zones in the block, based on RDI's, reach as low as 2-10 ohm-m and bedrock values reach as high as approx. 1500-4000 ohm-m. The estimated depth of the top of the anomalous zones, based on RDI, varies from

approximately near surface to ~100 m and maximum depths of investigation (DOI) vary between approx. 275m->700 m.

A3 Ringwood: The Ringwood block displays a gradual, regional-like increase in magnetic intensity from northeast towards the south-west, with smaller, more localized, and irregularly magnetic highs located near the north-east and south-west corners of the block. CVG magnetic derivatives define narrower lineament trends throughout the block that indicate a gradual change in geologic strike from NW-SE in the northern part to NE-SW in the southern part, suggesting a symmetric, EW-axial, recumbent antiformal fold, open to the west. . Electromagnetically, the Ringwood block displays conductive and resistive units with similar structural trends as shown in the magnetics. Generally speaking, more resistive rocks are found in the western and northeastern parts of the block and more conductive units in the south-west and east-central parts of the block. These conductive anomalies mainly subcrop and are banded to stratigraphic like and do not appear to have magnetic association. Some of the larger, wider, and most conductive features possibly relate to conductive overburden or pelitic sediments or else porewater salinity. Conductive anomalies in the Ringwood block feature EM dB_z/dt time constants in the 0.6 to 1.80 ms range, indicating moderate to high conductivities. Based on RDI imaging results, apparent resistivities reach as low <1 ohm-m and bedrock values reach approx. 1k-2.5k ohm-m. The estimated depth of the top of the anomalous zones, based on RDI, varies from approximately near surface to ~50 m. Maximum depths of investigation (DOI) vary between approx. 100-600 m.

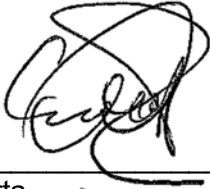
A4 No.5 Bore: Magnetically, the No.5 Bore block features a fairly well-defined, elongate northeast-southwest magnetic high anomaly that extends across the centre of the block. CVG magnetic derivatives indicate that this high is also flanked by alternating NW-SE trending magnetic low and high susceptibility units. Electromagnetically, the northwestern half of the block is more resistive than the southeastern half, with trends in the same orientation as the magnetic anomalies (south-west to north-east). The EM results suggest that the central magnetic high is mainly conductive, whereas other conductive anomalies in the northwestern and southeastern part of the block are non-magnetic. The near-surface nature of the EM anomalies suggests they could also be related to conductive overburden or pelitic sediments or else possibly due porewater salinity. The conductive anomalies in the No.5 Bore block feature EM dB_z/dt time constants in the 0.9 to 1.44 ms range, which indicates high conductivities. Based on RDI imaging results, apparent resistivities of anomalous zones in the block are as low as <1 ohm-m and bedrock values reach as high as approx. 700-1000 ohm-m. The estimated depth of the top of the anomalous zones varies from ~50-100 m and maximum depths of investigation (DOI) vary from approx. 150-375 m.

A5 Kay Creek: The Kay Creek block shows a partially defined NW-SE trending magnetic high at the northeastern end of the block and a partially-defined, NW-SE elongate magnetic low in the southwestern half of the block. Magnetic derivatives also reveal numerous short (<300 - 600 m) strike-length, alternating magnetic highs and lows in the southwestern half of the block. Electromagnetically, the southwestern half block features a well-defined, large area (~ 2×5 km) conductive unit striking NE-SW, and therefore discordant with the magnetic trends, but possibly related to conductive overburden or pelitic sediments; whereas in the northeastern end of the block, conductive and resistive features that appear to be NW-SE trending and therefore concordant with magnetic results. The conductive anomalies in the Kay Creek block feature EM dB_z/dt time constants in the 0.4 to 0.66 ms range, indicating moderate conductivities. The

block's apparent resistivities in anomalous zones are as low as ~5-10 ohm-m and bedrock resistivity high values reach approx. 1200-1800 ohm-m. The estimated depth of the top of the anomalous zones, based on RDI imaging, varies from approximately near surface to ~125 m and maximum depths of investigation (DOI) vary between approx. 350-550 m.

Based on the VTEM electromagnetic and aeromagnetic results obtained, we recommend that more advanced, integrated interpretation be performed on these geophysical data prior to ground follow-up. This should include EM anomaly picking and Maxwell plate modeling of major anomalies of interest. 1D EM inversion may assist in accurately mapping layered earth resistivity parameters of the conductive cover and the bedrock resistivities across the block. 3D MVI (magnetic vector inversions) combined with ML (machine learning) assisted analyses may reveal the spatial correlations between the bedrock conductors and related magnetic bodies, as well as geological lithology. Semi-automated CET-type magnetic lineament analysis will provide additional information on major structural trends on the property.

Respectfully submitted²,



Marta Orta
UTS Geophysics



Gaurav Nailwal
UTS Geophysics



Andrea Reman
UTS Geophysics



Emily Data, P.Ge
UTS Geophysics



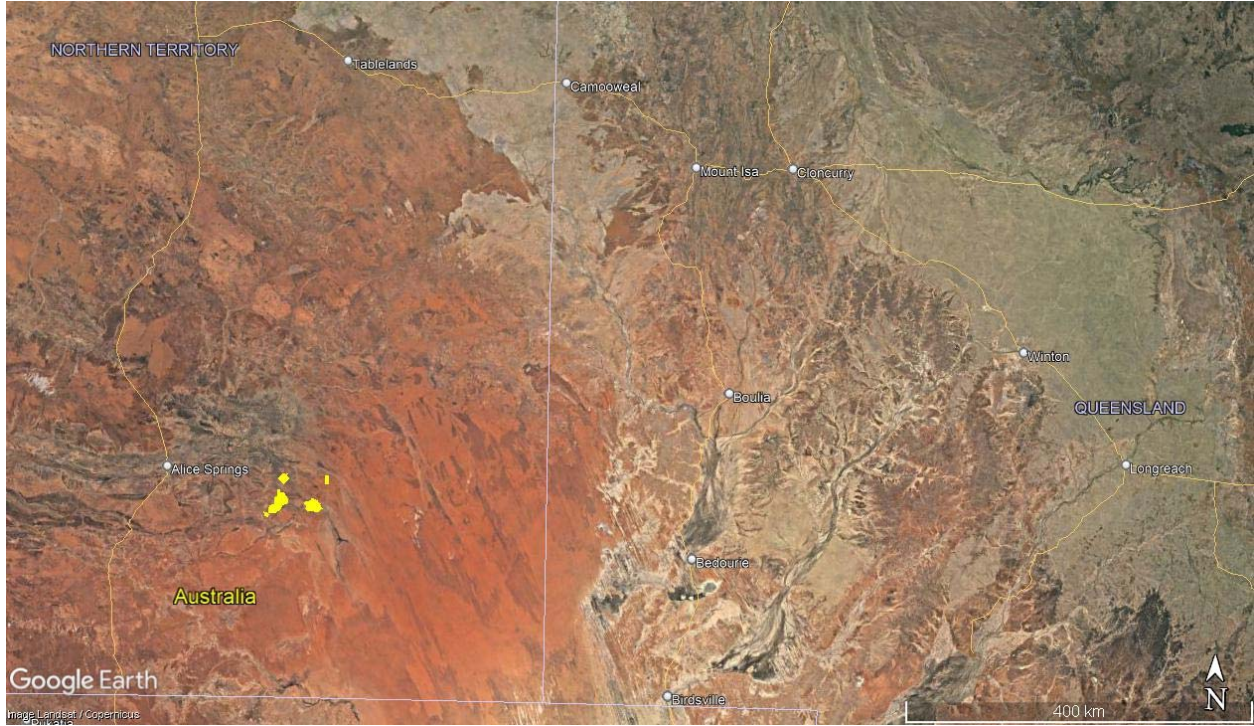
Jean M. Legault, M.Sc.A., P.Eng, P.Ge
UTS Geophysics

August 2021

² Final data processing of the EM and magnetic data was carried out by Andrea Reman, under the supervision of Emily Data & Jean M. Legault, Chief Geophysicist.

APPENDIX A

SURVEY BLOCK LOCATION MAP



Survey Overview of the Survey Area

APPENDIX B

SURVEY BLOCK COORDINATES (WGS 84, UTM Zone 53 South)

Arumbera (A1)	
X	Y
563186	7359746
567372	7359746
567372	7368240
563186	7368240

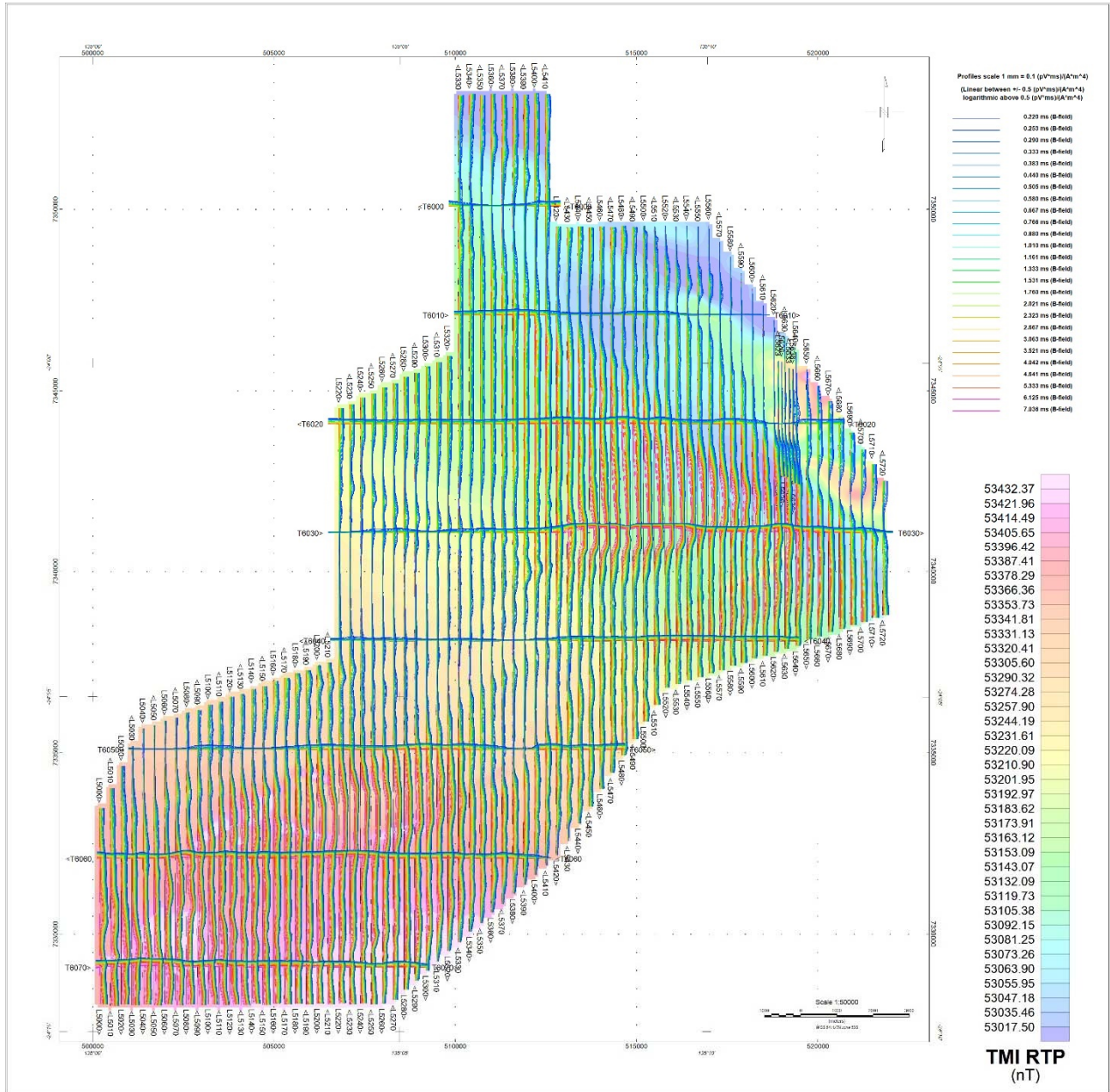
Ringwood (A3)	
X	Y
510047	7353199
512523	7353199
512591	7349553
516932	7349604
521798	7342516
521815	7338751
515745	7336768
511980	7331291
508284	7328137
500144	7328052
500127	7333495
501365	7335716
506605	7337598
506656	7344602
509928	7346128

No5 Bore (A4)	
X	Y
494296	7328743
496067	7327740
496435	7328409
500078	7326326
498329	7323329
494742	7325423
495889	7327384
494051	7328431

South Numery (A2)	
X	Y
540387	7338955
542732	7341233
543559	7340406
544251	7341115
545111	7340271
549059	7344118
555756	7339344
558675	7333321
554491	7329086
542311	7331381
542193	7337268

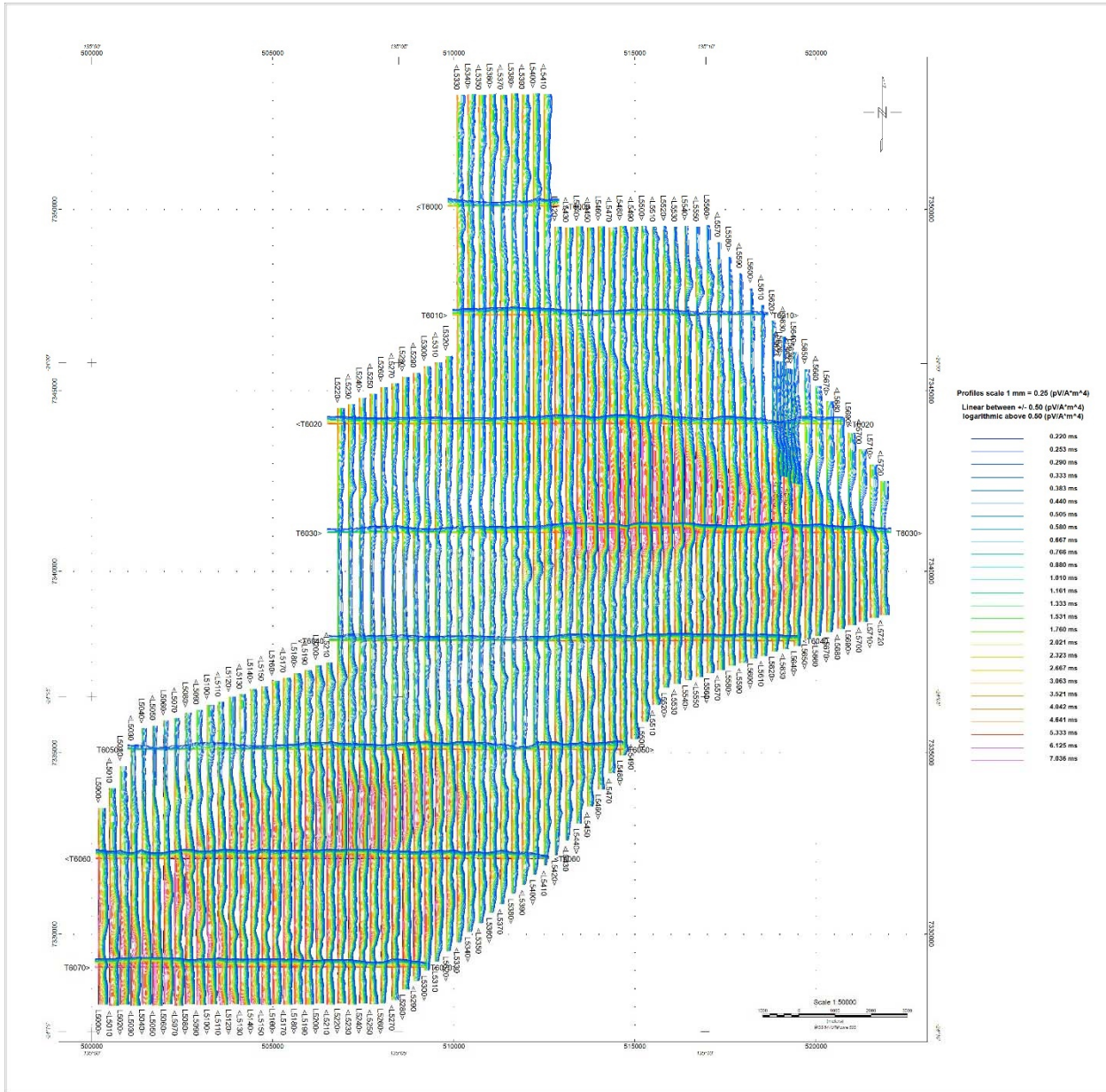
Kay Creek (A5)	
X	Y
517068	7371395
519293	7369284
521656	7371578
522069	7371165
519775	7368734
523193	7365408
517252	7359466
511127	7365591

APPENDIX C - GEOPHYSICAL MAPS¹ - A3 RINGWOOD

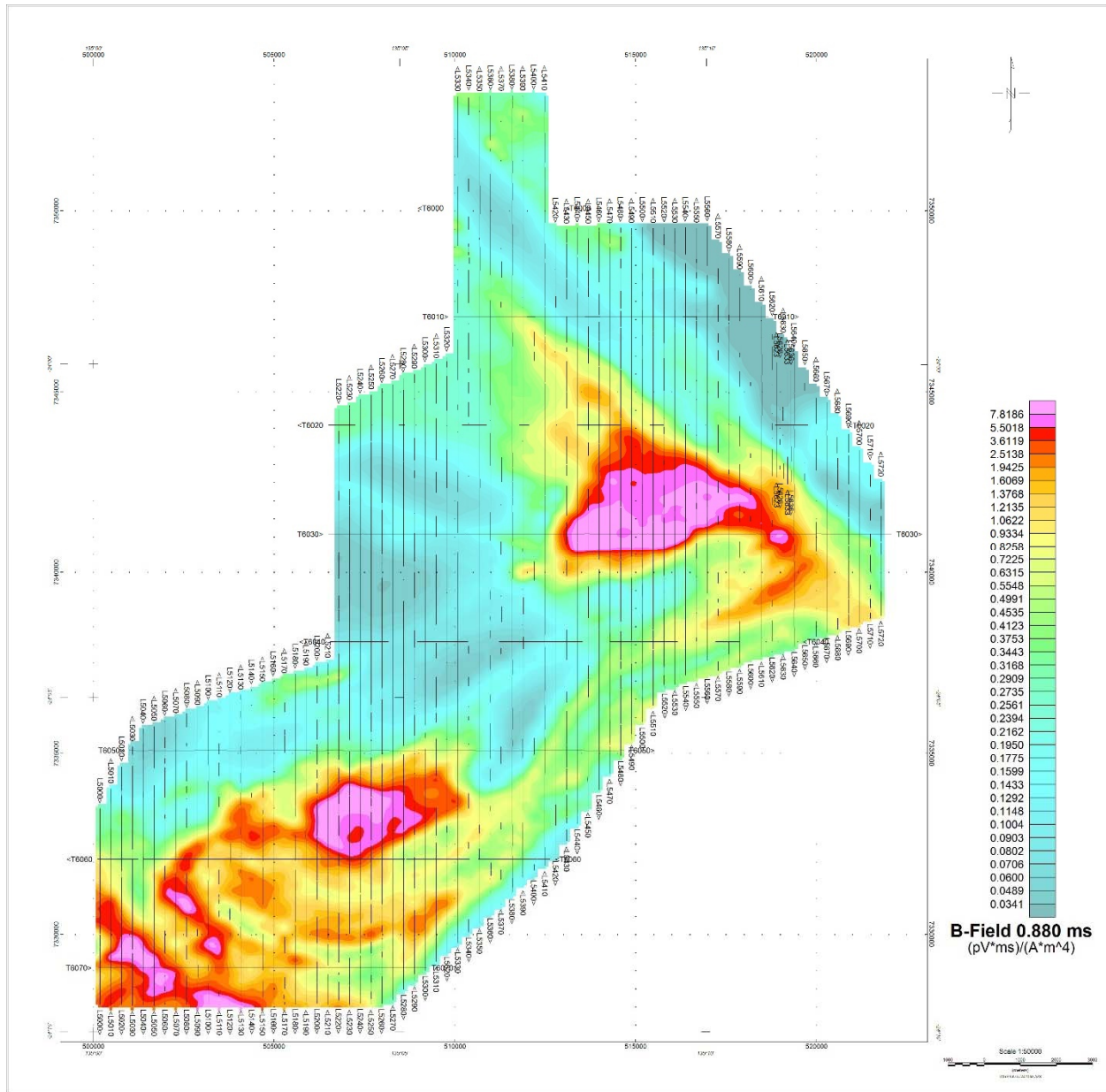


A3 Ringwood: B-field profiles Z Component, Time Gates 0.220 – 7.036 ms in linear – logarithmic scale over Total Magnetic Intensity, Reduced to Pole colour image (RTP)

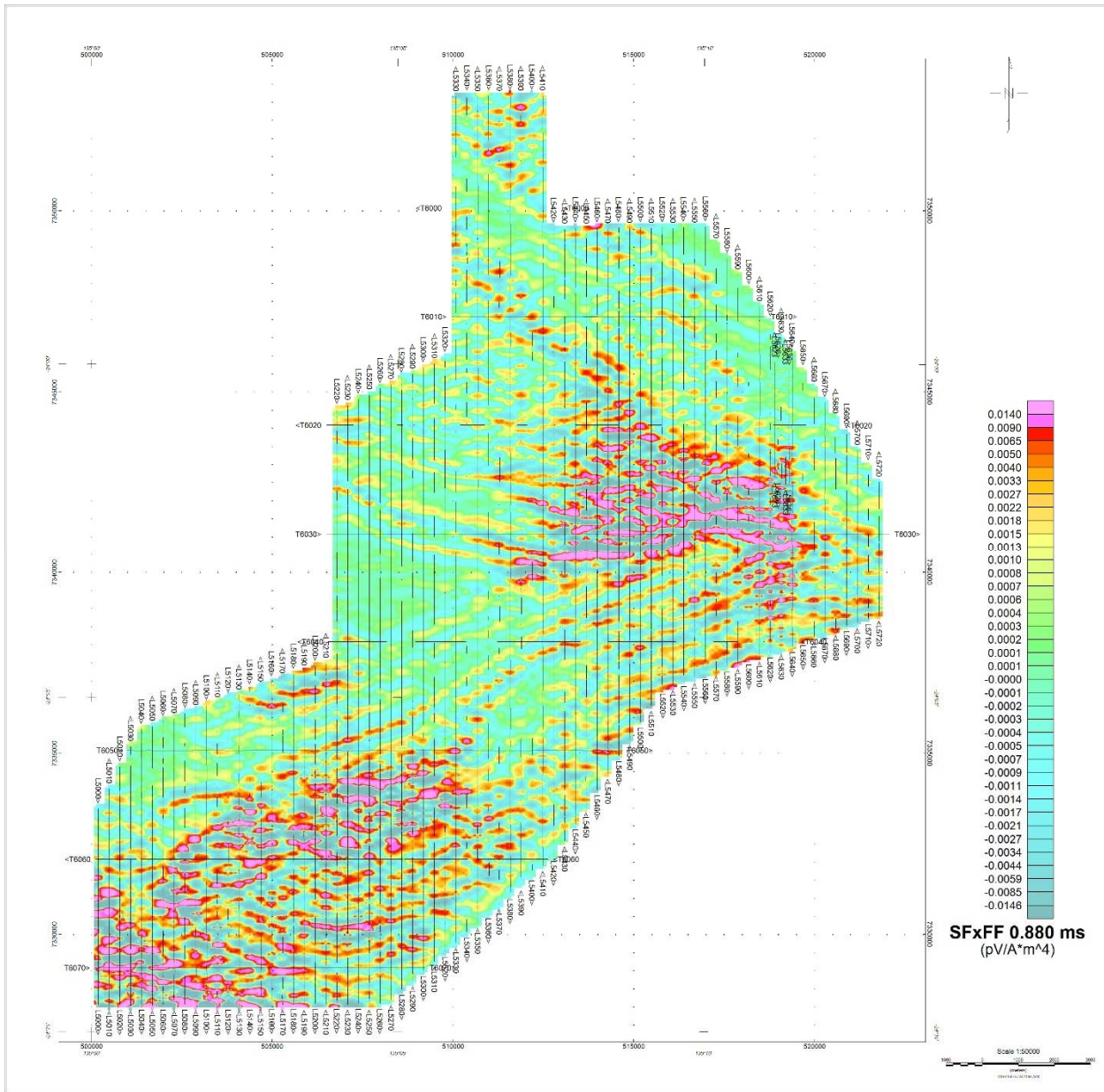
¹ Full size geophysical maps are also available in PDF format on the final DVD



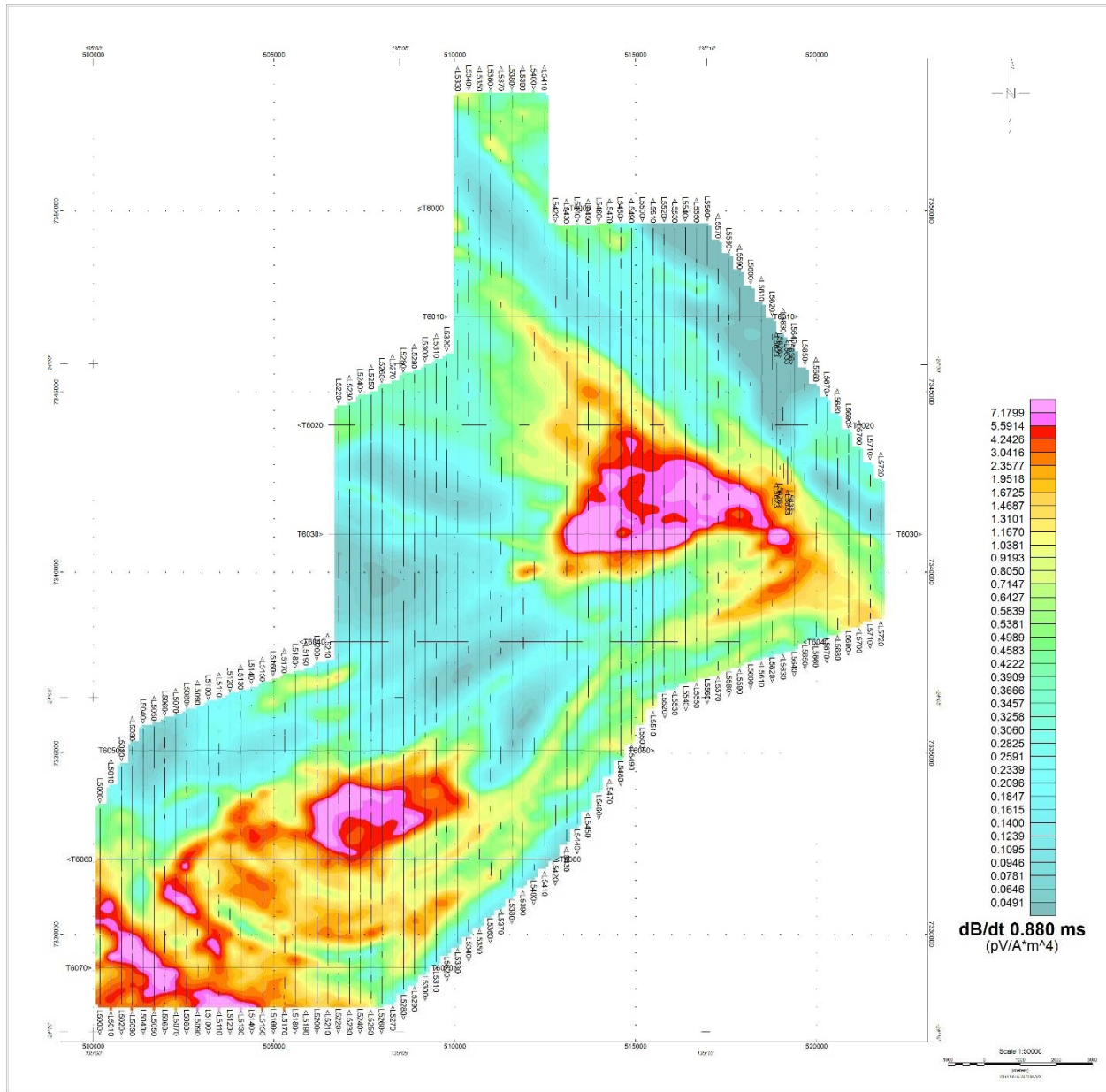
A3 Ringwood: dB/dt profiles Z Component, Time Gates 0.220 – 7.036 ms in linear – logarithmic scale



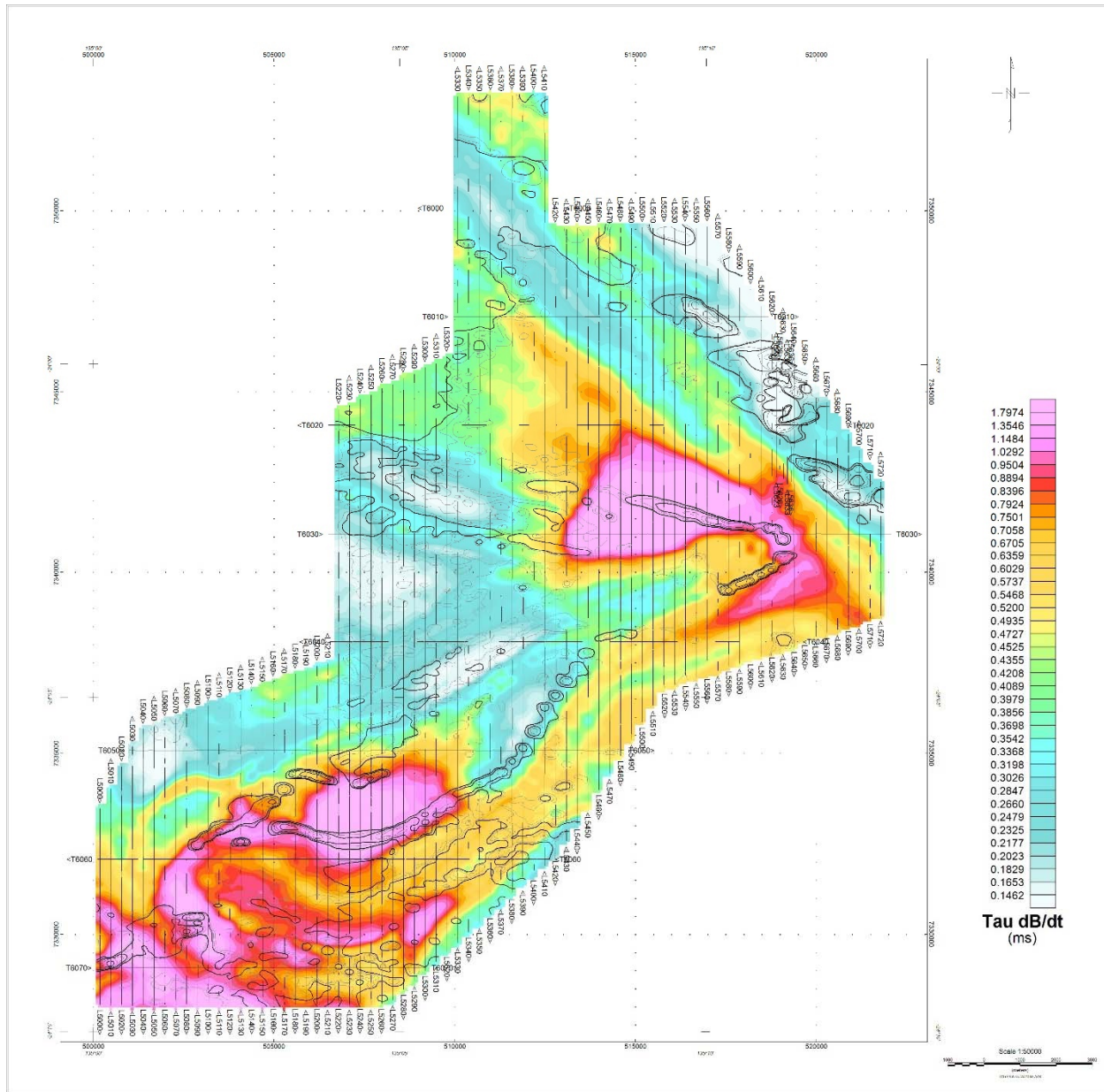
A3 Ringwood: B-field Z Component Channel 30, Time Gate 0.880 ms



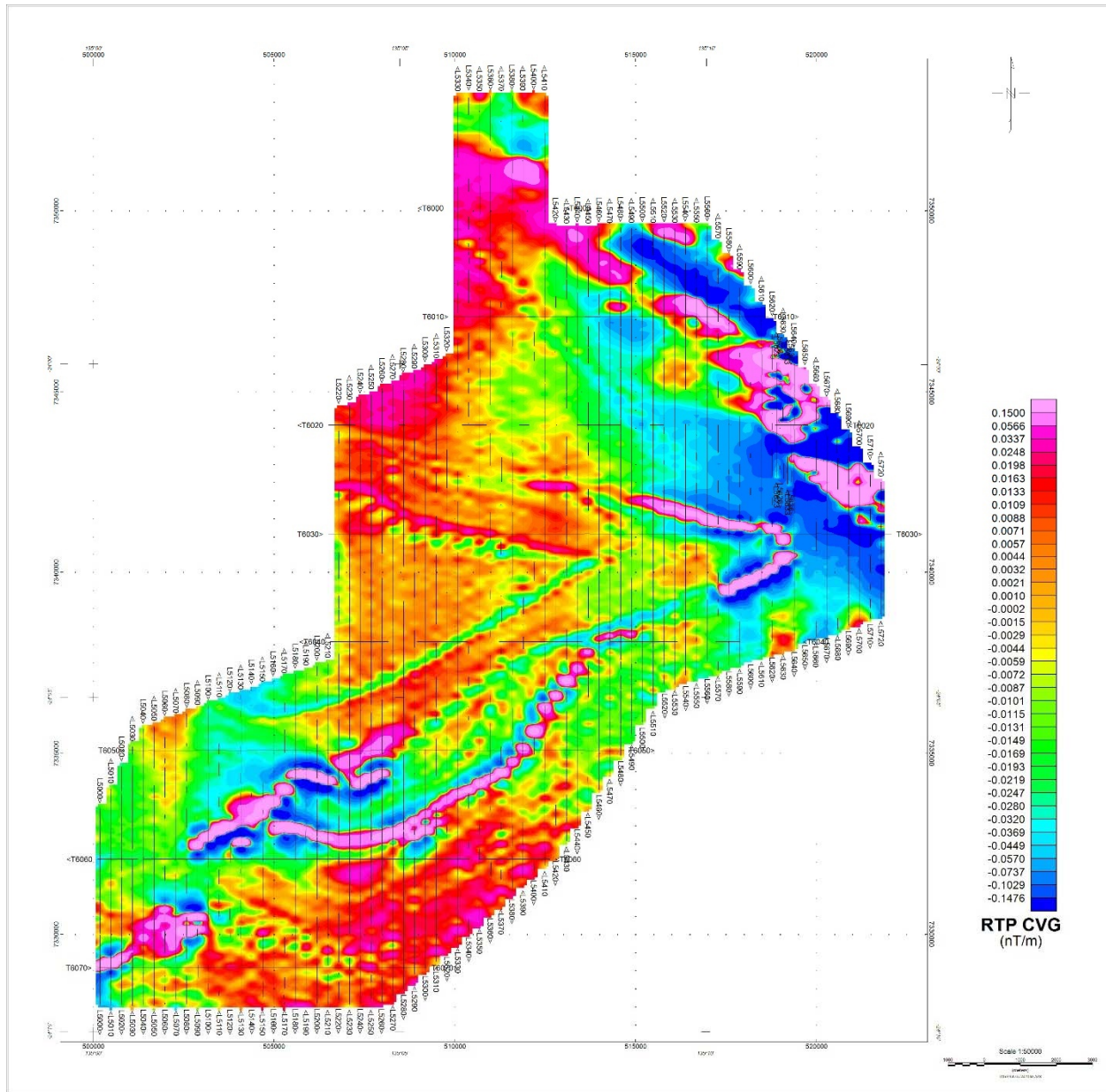
A3 Ringwood: Fraser Filtered dB/dt X Component, Channel 30, Time Gate 0.880 ms



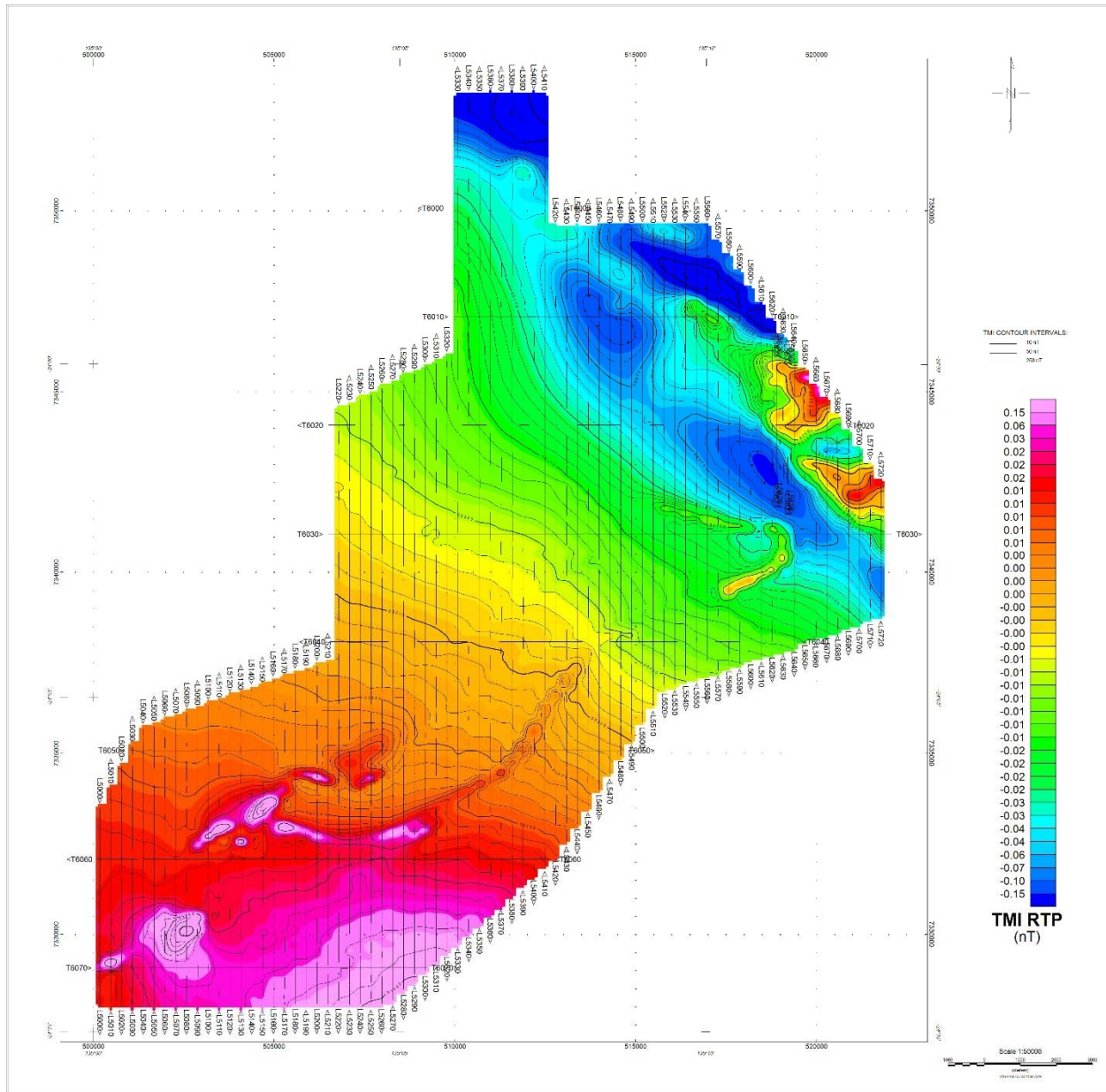
A3 Ringwood: dB/dt Z Component Channel 30 (Time Gate 0.880 ms)



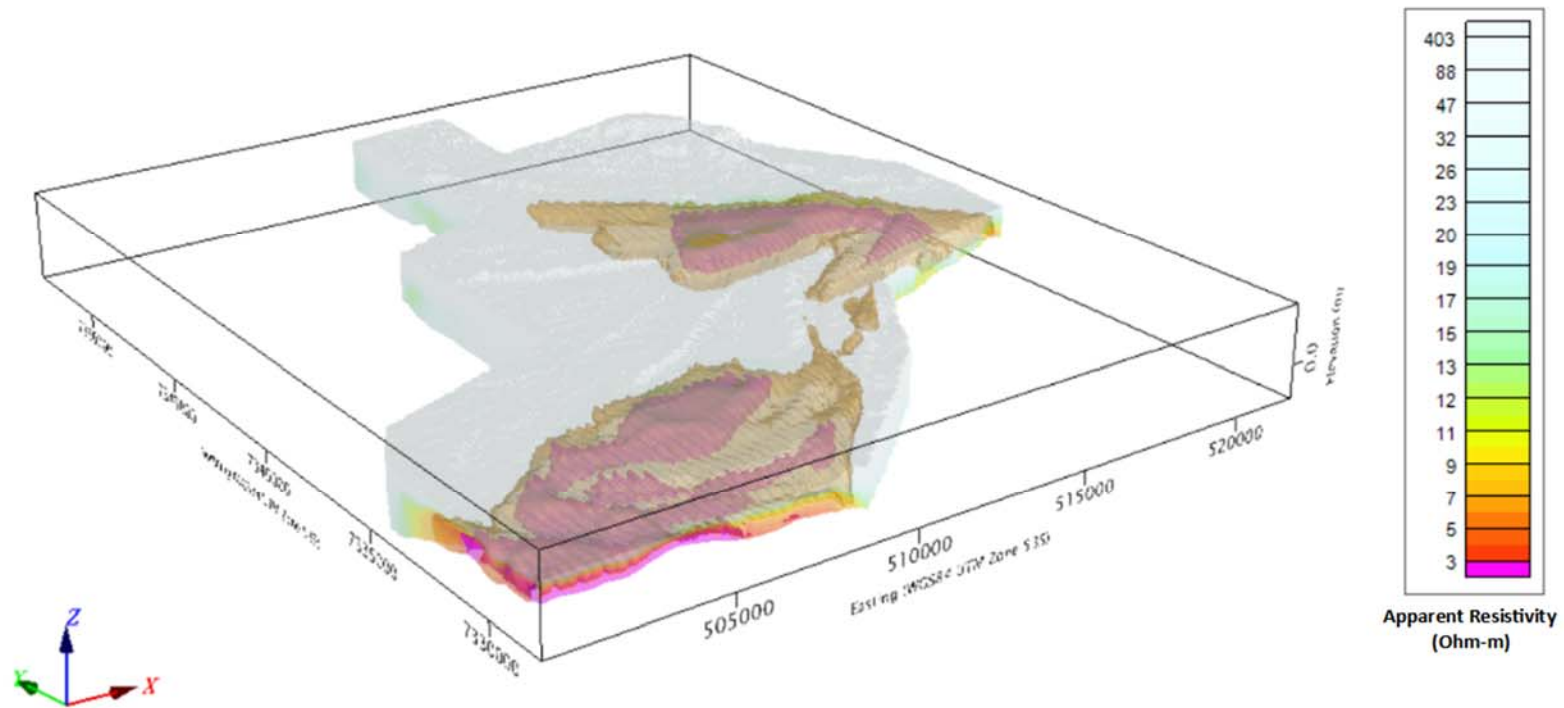
A3 Ringwood: Z-component dB/dt Calculated Time Constant (Tau) with Calculated Vertical Derivative, Reduced to Pole (CVG_RTP) contours



A3 Ringwood: Calculated Vertical Gradient (CVG) Reduced to Pole (RTP)



A3 Ringwood: Total Magnetic Intensity (TMI) Reduced to Pole (RTP)



3D View of Apparent Resistivity Depth Images (RDI) Voxel – A3 Ringwood

APPENDIX D

GENERALIZED MODELING RESULTS OF THE VTEM™ SYSTEM

Introduction

The VTEM™ system is based on a concentric or central loop design, whereby, the receiver is positioned at the centre of a transmitter loop that produces a primary field. The wave form is a bi-polar, modified square wave with a turn-on and turn-off at each end.

During turn-on and turn-off, a time varying field is produced (dB/dt) and an electro-motive force (emf) is created as a finite impulse response. A current ring around the transmitter loop moves outward and downward as time progresses. When conductive rocks and mineralization are encountered, a secondary field is created by mutual induction and measured by the receiver at the centre of the transmitter loop.

Efficient modeling of the results can be carried out on regularly shaped geometries, thus yielding close approximations to the parameters of the measured targets. The following is a description of a series of common models made for the purpose of promoting a general understanding of the measured results.

A set of models has been produced for the UTS VTEM™ system dB/dT Z and X components (see models D1 to D15). The Maxwell™ modeling program (EMIT Technology Pty. Ltd. Midland, WA, AU) used to generate the following responses assumes a resistive half-space. The reader is encouraged to review these models, so as to get a general understanding of the responses as they apply to survey results. While these models do not begin to cover all possibilities, they give a general perspective on the simple and most commonly encountered anomalies.

As the plate dips and departs from the vertical position, the peaks become asymmetrical.

As the dip increases, the aspect ratio (Min/Max) decreases and this aspect ratio can be used as an empirical guide to dip angles from near 90° to about 30°. The method is not sensitive enough where dips are less than about 30°.

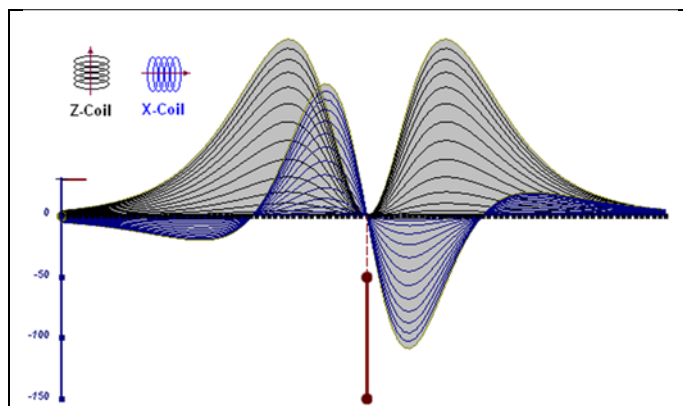


Figure D-1: vertical thin plate

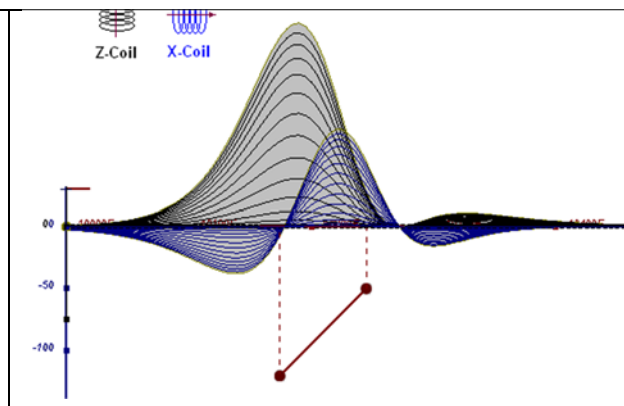


Figure D-2: inclined thin plate

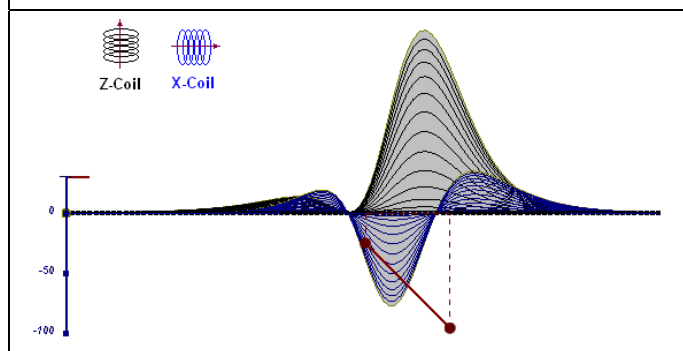


Figure D-3: inclined thin plate

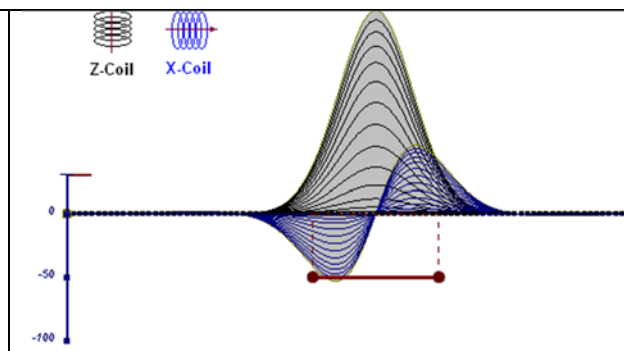


Figure D-4: horizontal thin plate

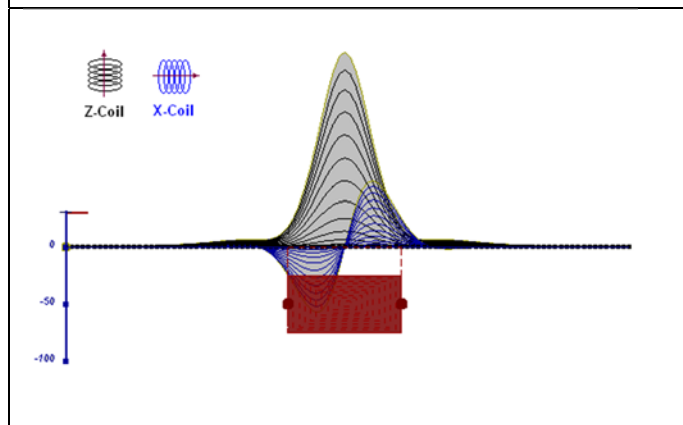


Figure D-5: horizontal thick plate (linear scale of the response)

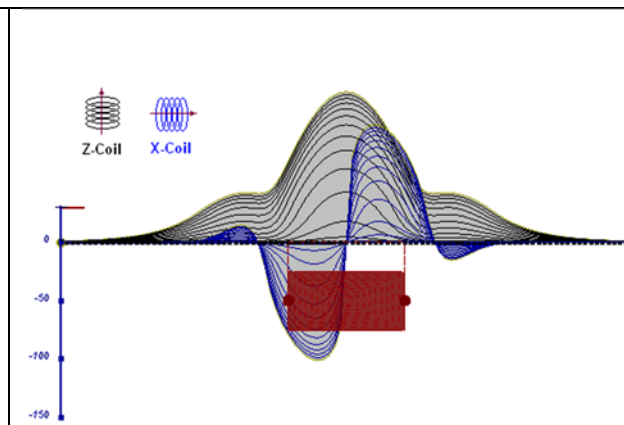


Figure D-6: horizontal thick plate (log scale of the response)

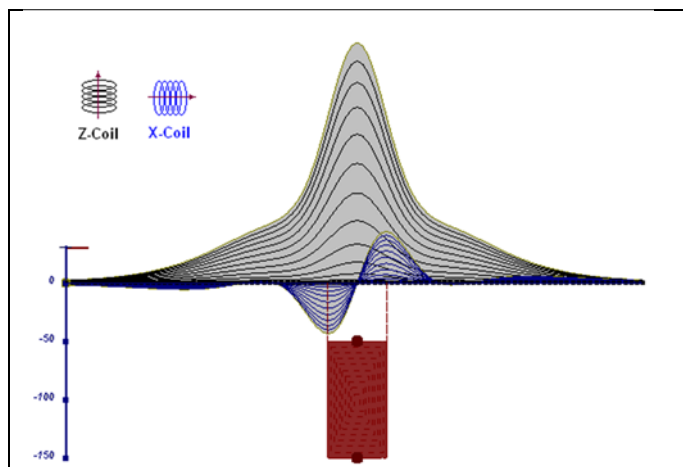


Figure D-7: vertical thick plate (linear scale of the response). 50 m depth

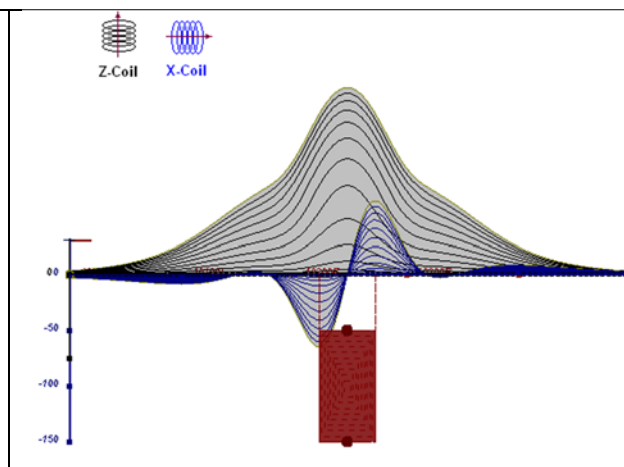


Figure D-8: vertical thick plate (log scale of the response). 50 m depth

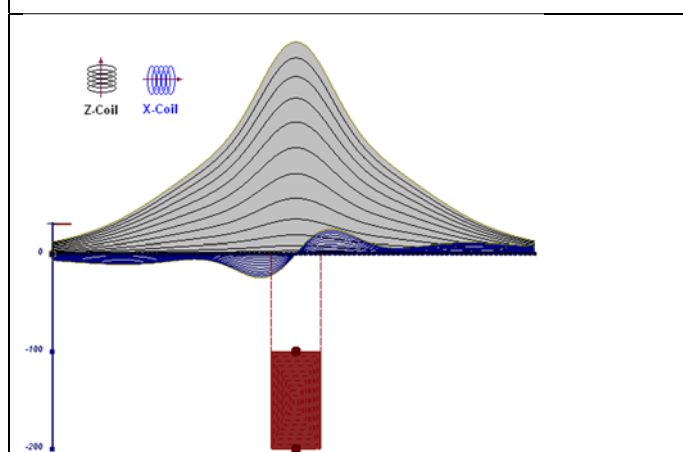


Figure D-9: vertical thick plate (linear scale of the response). 100 m depth

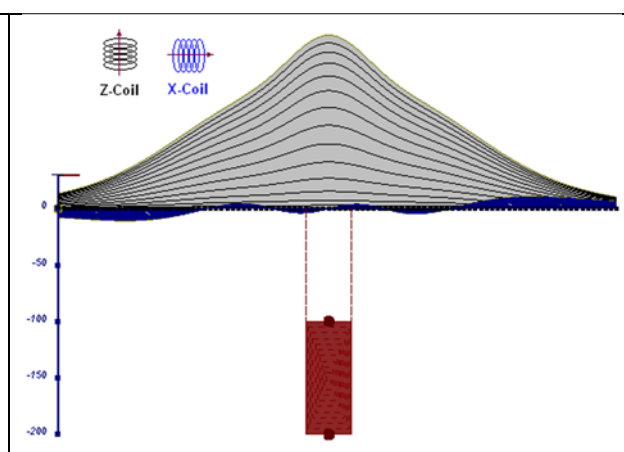


Figure D-10: vertical thick plate (linear scale of the response). Depth/thickness=2.5

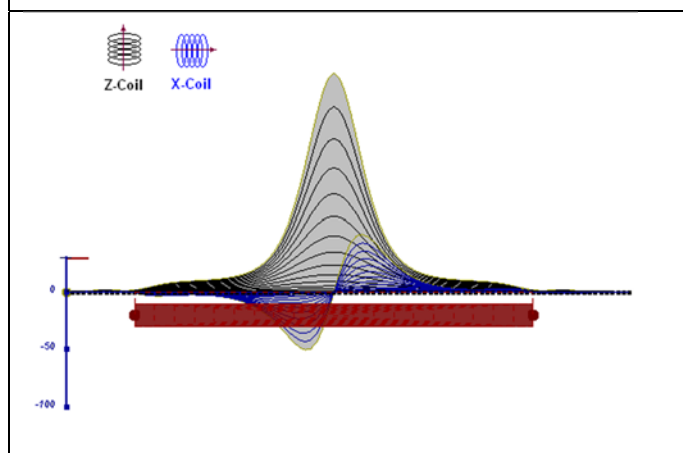


Figure D-10: horizontal thick plate (linear scale of the response)

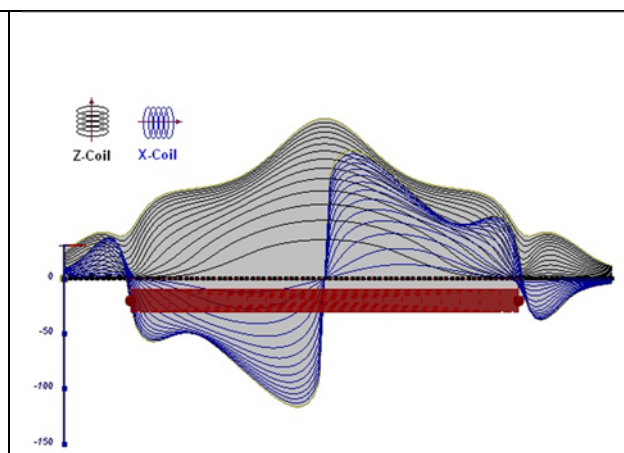


Figure D-11: horizontal thick plate (log scale of the response)

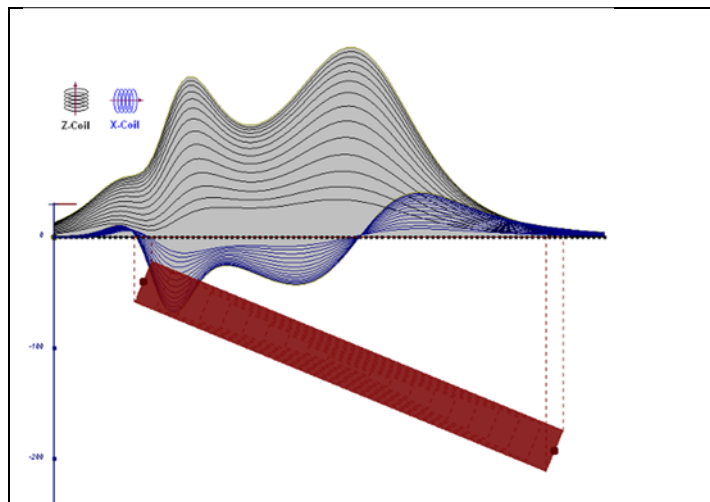


Figure D-12: inclined long thick plate

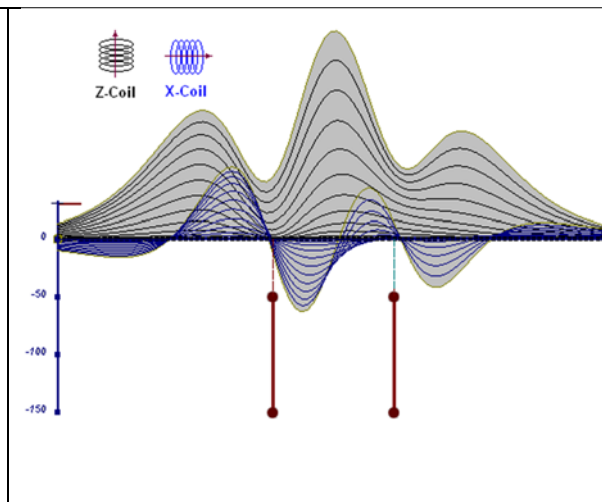


Figure D-13: two vertical thin plates

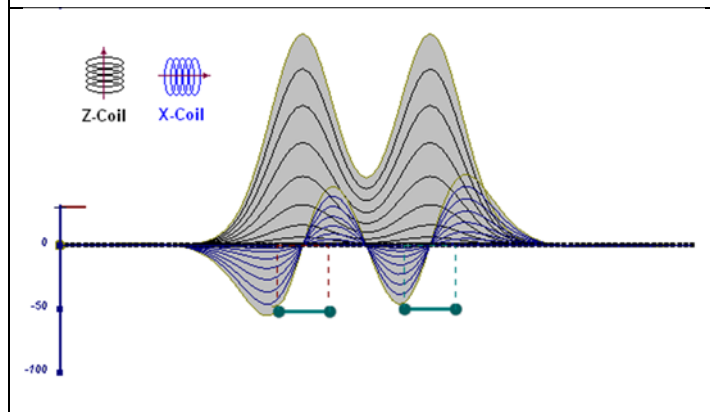


Figure D-14: two horizontal thin plates

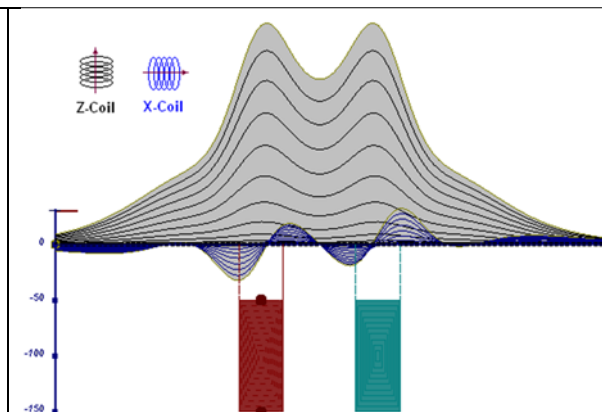


Figure D-15: two vertical thick plates

The same type of target but with different thickness, for example, creates different form of the response:

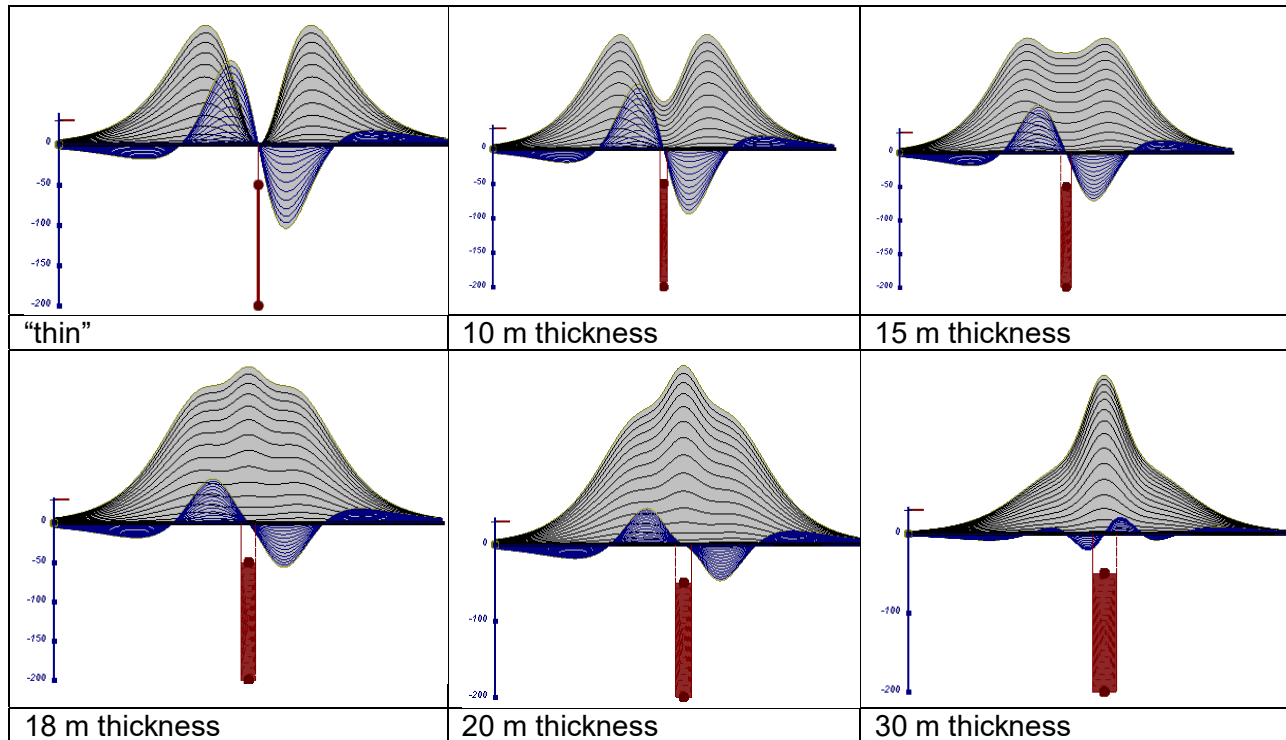


Figure D-16: Conductive vertical plate, depth 50 m, strike length 200 m, depth extend 150 m.

Alexander Prikhodko, PhD, P.Ge
UTS Ltd.

September 2010

APPENDIX E

EM TIME CONSTANT (TAU) ANALYSIS

Estimation of time constant parameter¹ in transient electromagnetic method is one of the steps toward the extraction of the information about conductances beneath the surface from TEM measurements.

The most reliable method to discriminate or rank conductors from overburden, background or one and other is by calculating the EM field decay time constant (TAU parameter), which directly depends on conductance despite their depth and accordingly amplitude of the response.

Theory

As established in electromagnetic theory, the magnitude of the electro-motive force (emf) induced is proportional to the time rate of change of primary magnetic field at the conductor. This emf causes eddy currents to flow in the conductor with a characteristic transient decay, whose Time Constant (Tau) is a function of the conductance of the survey target or conductivity and geometry (including dimensions) of the target. The decaying currents generate a proportional secondary magnetic field, the time rate of change of which is measured by the receiver coil as induced voltage during the Off time.

The receiver coil output voltage (e_0) is proportional to the time rate of change of the secondary magnetic field and has the form,

$$e_0 \propto (1 / \tau) e^{-t/\tau}$$

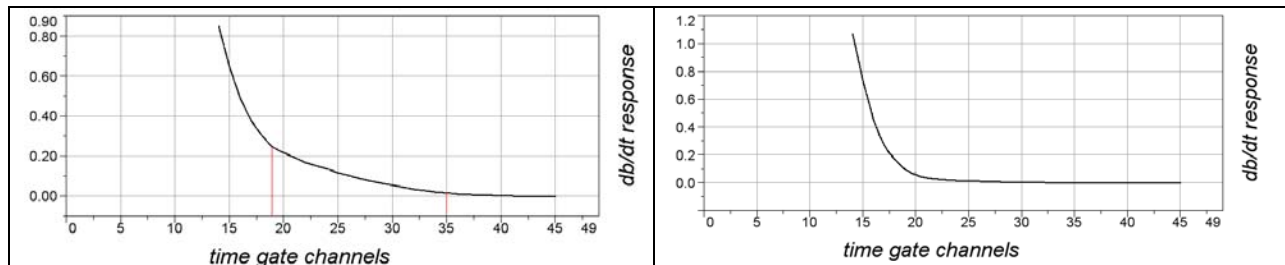
Where,

$\tau = L/R$ is the characteristic time constant of the target (TAU)

R = resistance

L = inductance

From the expression, conductive targets that have small value of resistance and hence large value of τ yield signals with small initial amplitude that decays relatively slowly with progress of time. Conversely, signals from poorly conducting targets that have large resistance value and small τ , have high initial amplitude but decay rapidly with time¹ (Figure E-1).



¹ McNeill, JD, 1980, "Applications of Transient Electromagnetic Techniques", Technical Note TN-7 page 5, Geonics Limited, Mississauga, Ontario.

Figure E-1: Left – presence of good conductor, right – poor conductor.

EM Time Constant (Tau) Calculation

The EM Time-Constant (TAU) is a general measure of the speed of decay of the electromagnetic response and indicates the presence of eddy currents in conductive sources as well as reflecting the “conductance quality” of a source. Although TAU can be calculated using either the measured dB/dt decay or the calculated B-field decay, dB/dt is commonly preferred due to better stability (S/N) relating to signal noise. Generally, TAU calculated on base of early time response reflects both near surface overburden and poor conductors whereas, in the late ranges of time, deep and more conductive sources, respectively. For example, early time TAU distribution in an area that indicates conductive overburden is shown in Figure 2.

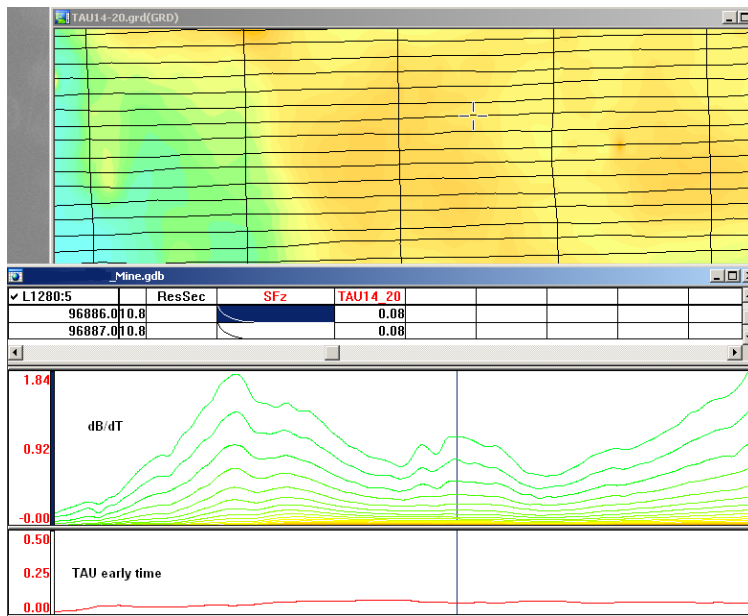


Figure E-2: Map of early time TAU. Area with overburden conductive layer and local sources.

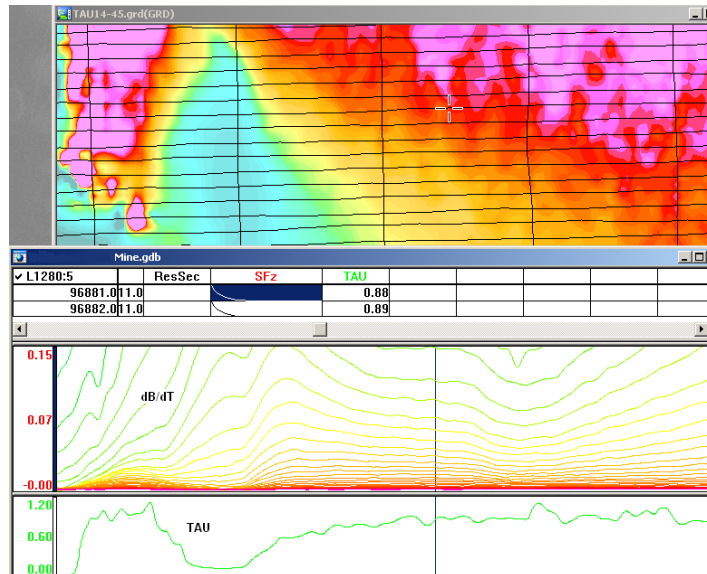


Figure E-3: Map of full time range TAU with EM anomaly due to deep highly conductive target.

There are many advantages of TAU maps:

- TAU depends only on one parameter (conductance) in contrast to response magnitude;
- TAU is integral parameter, which covers time range, and all conductive zones and targets are displayed independently of their depth and conductivity on a single map.
- Very good differential resolution in complex conductive places with many sources with different conductivity.
- Signs of the presence of good conductive targets are amplified and emphasized independently of their depth and level of response accordingly.

In the example shown in Figure 4 and 5, three local targets are defined, each of them with a different depth of burial, as indicated on the resistivity depth image (RDI). All are very good conductors, but the deeper target (number 2) has a relatively weak dB/dt signal yet also features the strongest total TAU (Figure 4). This example highlights the benefit of TAU analysis in terms of an additional target discrimination tool.

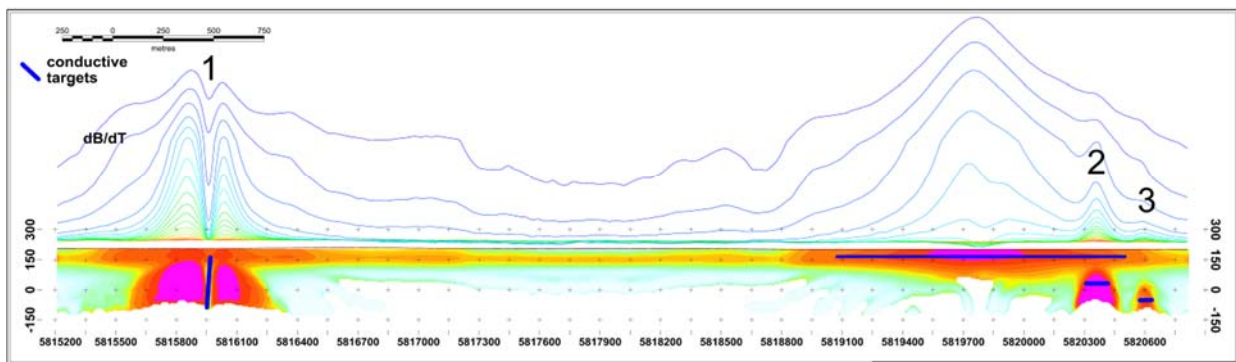


Figure E-4: dB/dt profile and RDI with different depths of targets.

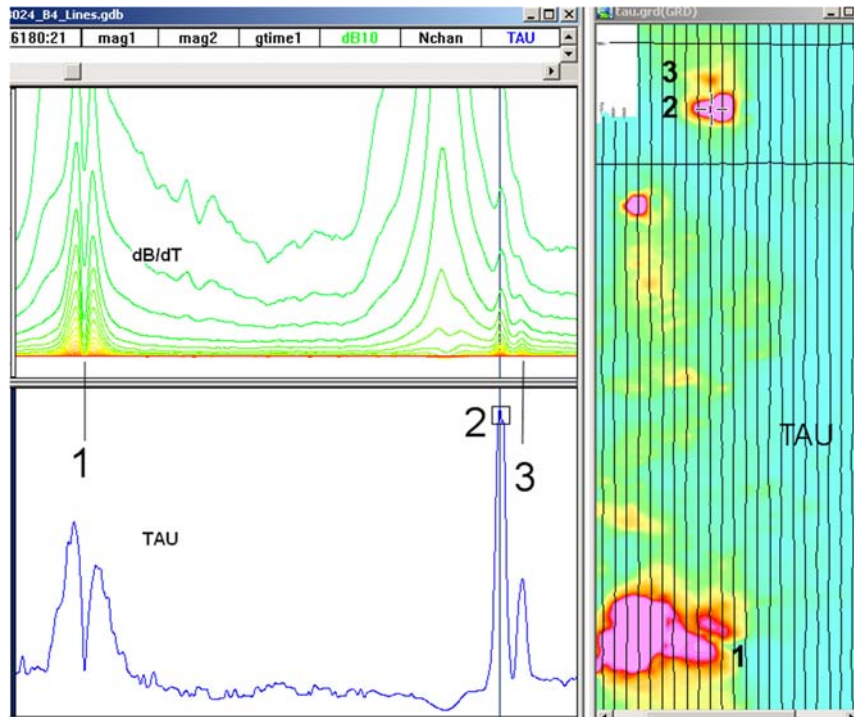


Figure E-5: Map of total TAU and dB/dt profile.

The EM Time Constants for dB/dt and B-field were calculated using the “sliding Tau” in-house program developed at UTS². The principle of the calculation is based on using of time window (4 time channels) which is sliding along the curve decay and looking for latest time channels which have a response above the level of noise and decay. The EM decays are obtained from all available decay channels, starting at the latest channel. Time constants are taken from a least square fit of a straight-line (log/linear space) over the last 4 gates above a pre-set signal threshold level (Figure F6). Threshold settings are pointed in the “label” property of TAU database channels. The sliding Tau method determines that, as the amplitudes increase, the time-constant is taken at progressively later times in the EM decay. Conversely, as the amplitudes decrease, Tau is taken at progressively earlier times in the decay. If the maximum signal amplitude falls below the threshold or becomes negative for any of the 4 time gates, then Tau is not calculated and is assigned a value of “dummy” by default.

² by A.Prikhodko

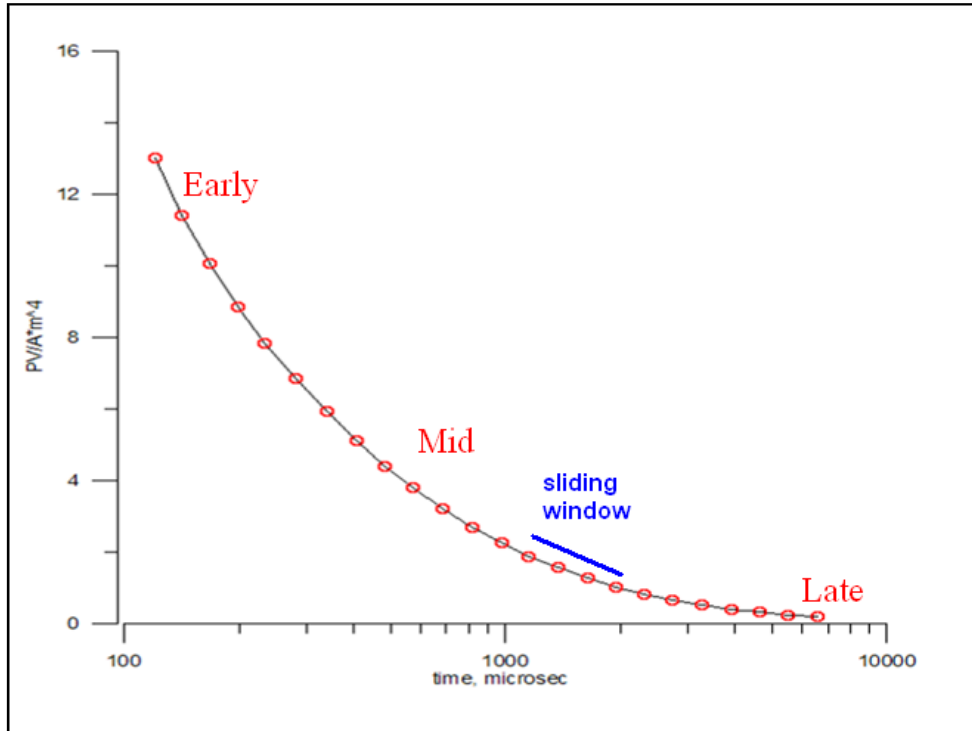


Figure E-6: Typical dB/dt decays of VTEM™ data

Alexander Prikhodko, PhD, P.Ge
UTS Ltd.

September 2010

APPENDIX F

TEM RESISTIVITY DEPTH IMAGING (RDI)

Resistivity depth imaging (RDI) is a technique used to rapidly convert EM profile decay data into an equivalent resistivity versus depth cross-section, by deconvolving the measured TEM data. The used RDI algorithm of Resistivity-Depth transformation is based on the scheme of the apparent resistivity transform of Maxwell A. Meju (1998)¹ and TEM response from a conductive half-space. The program is developed by Alexander Prikhodko and is depth-calibrated based on forward plate modeling for VTEM™ system configuration (Fig. 1-10).

RDIs provide reasonable indications of conductor relative depth and vertical extent, as well as accurate 1D layered-earth apparent conductivity/resistivity structure across VTEM™ flight lines. Approximate depth of investigation of a TEM system, image of secondary field distribution in half-space, effective resistivity, initial geometry, and position of conductive targets is the information obtained on the basis of the RDIs.

Maxwell forward modeling with RDI sections from the synthetic responses (VTEM™ system)

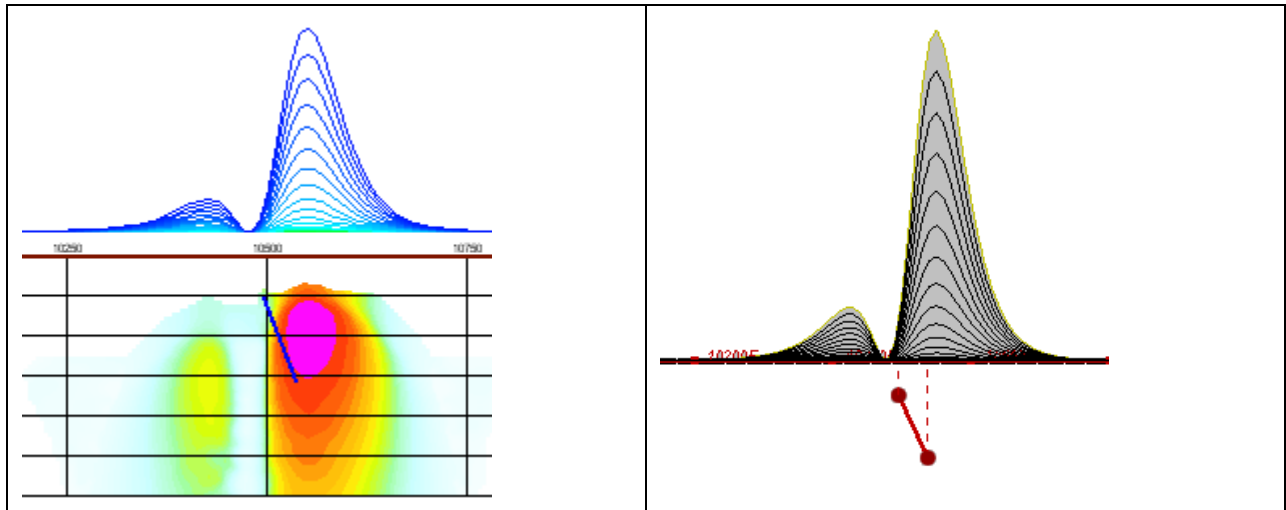


Figure F-1: Maxwell plate model and RDI from the calculated response for a conductive “thin” plate (depth 50 m, dip 65 degree, depth extend 100 m).

¹ Maxwell A. Meju, 1998, Short Note: A simple method of transient electromagnetic data analysis, *Geophysics*, **63**, 405–410.

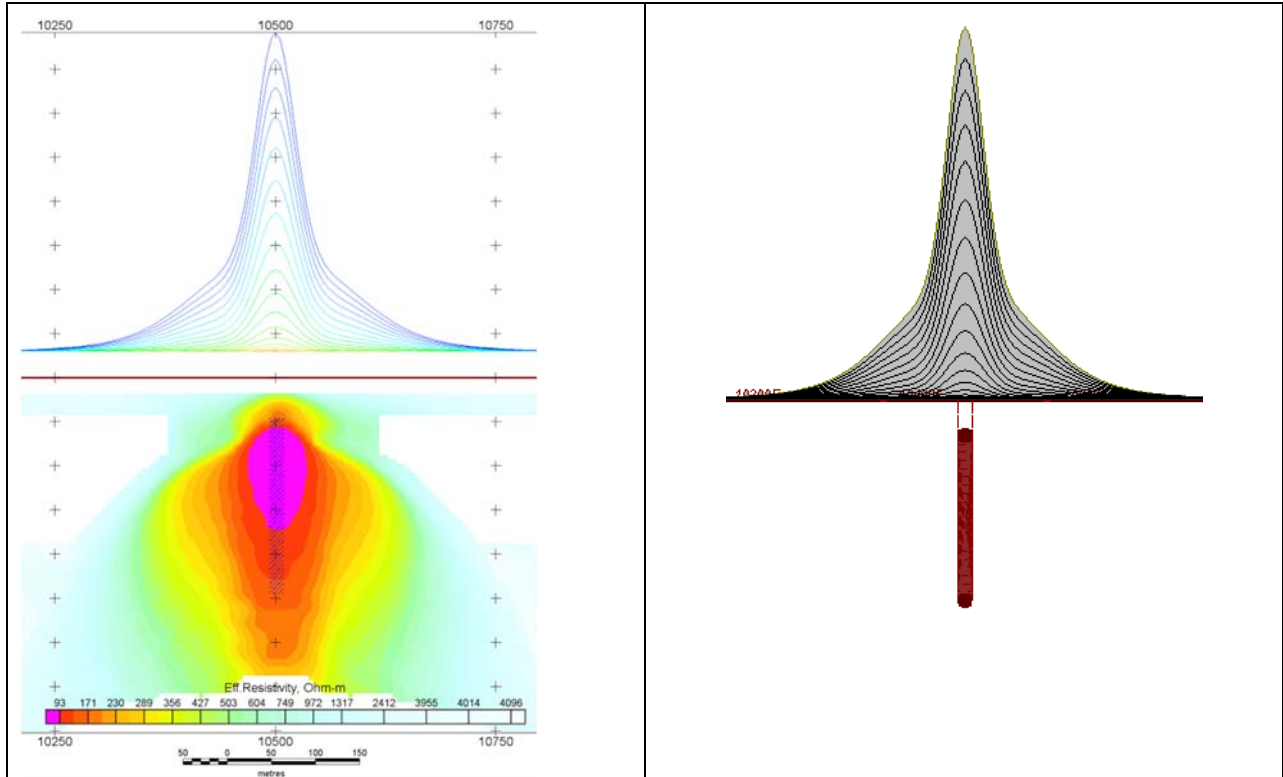


Figure F-2: Maxwell plate model and RDI from the calculated response for “thick” plate 18 m thickness, depth 50 m, depth extend 200 m).

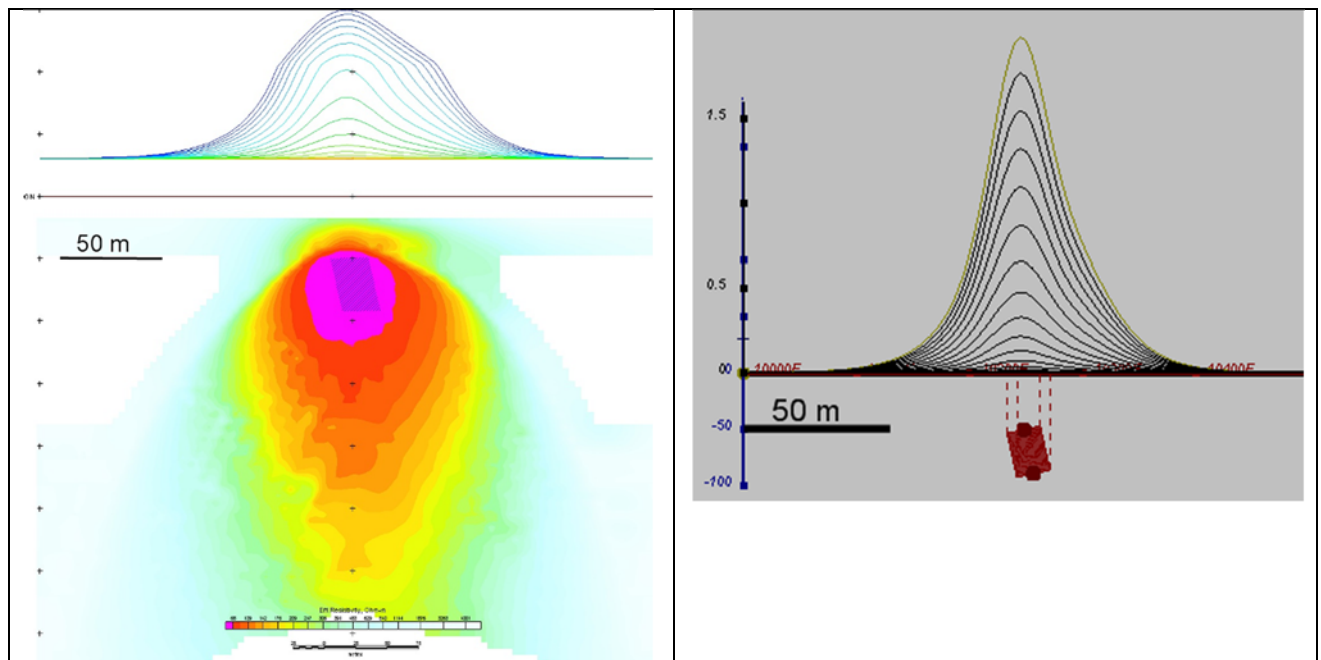


Figure F-3: Maxwell plate model and RDI from the calculated response for bulk (“thick”) 100 m length, 40 m depth extend, 30 m thickness

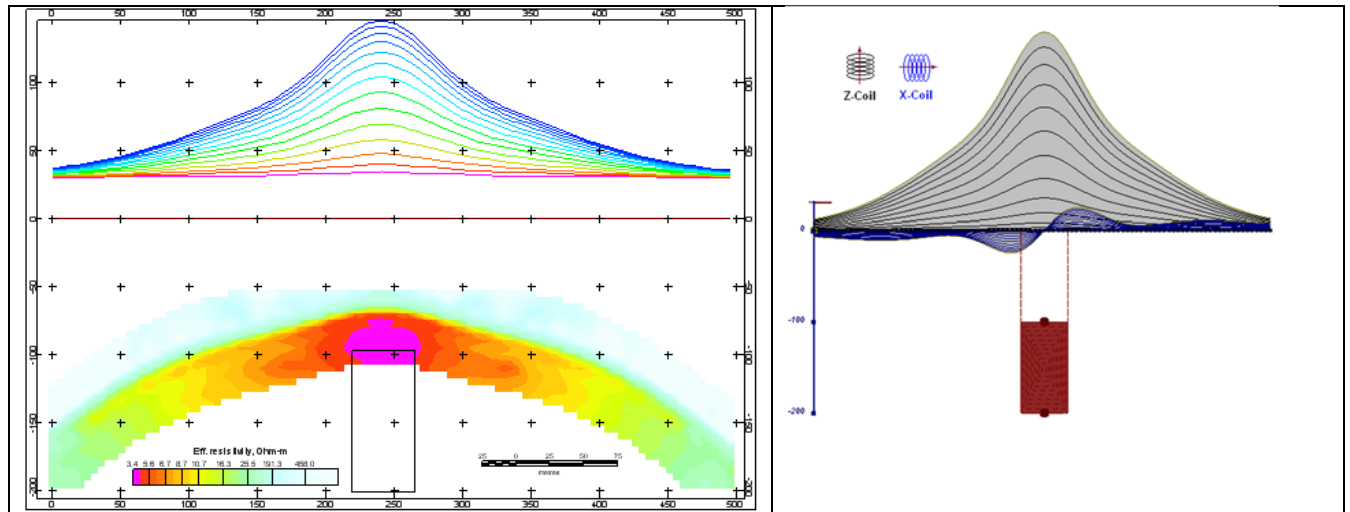


Figure F-4: Maxwell plate model and RDI from the calculated response for “thick” vertical target (depth 100 m, depth extend 100 m). 19-44 chan.

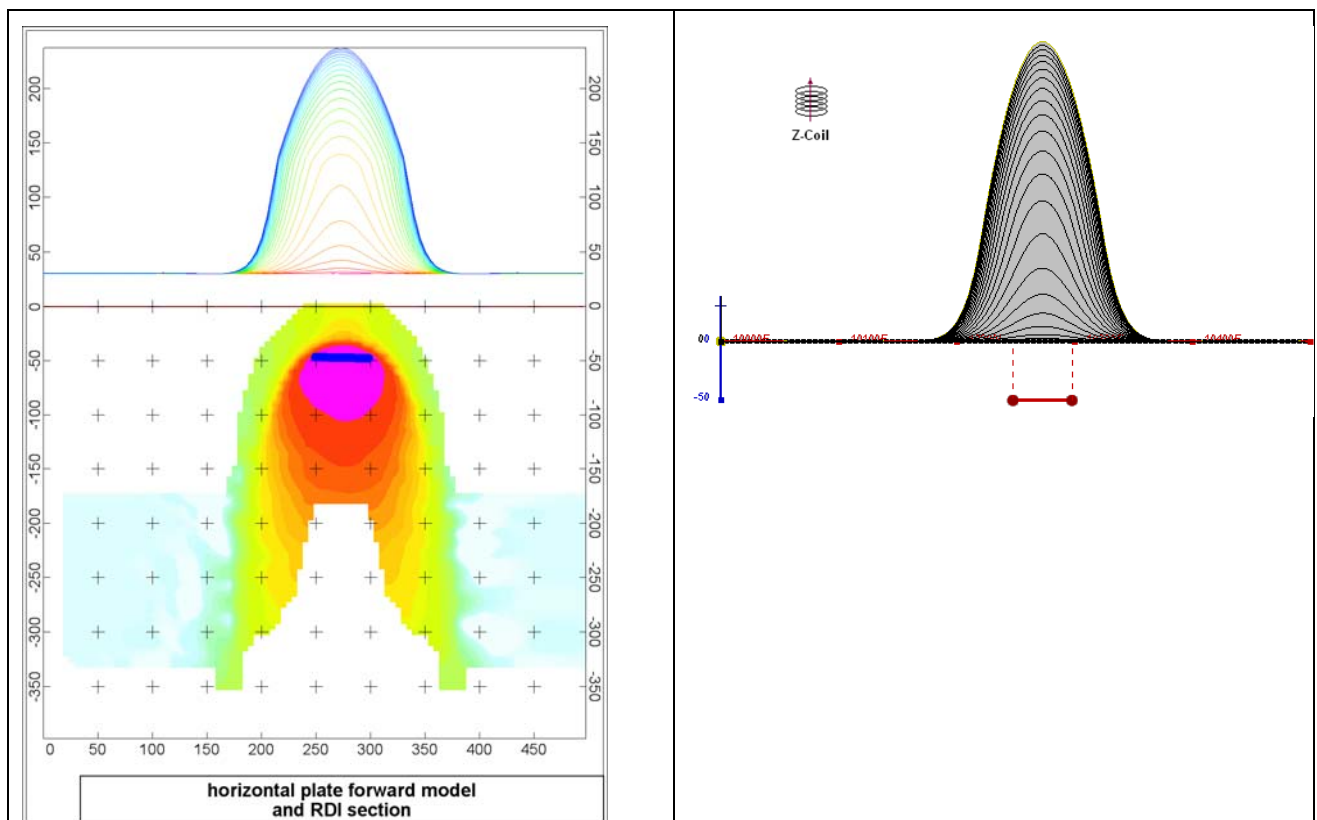


Figure F-5: Maxwell plate model and RDI from the calculated response for horizontal thin plate (depth 50 m, dim 50x100 m). 15-44 chan.

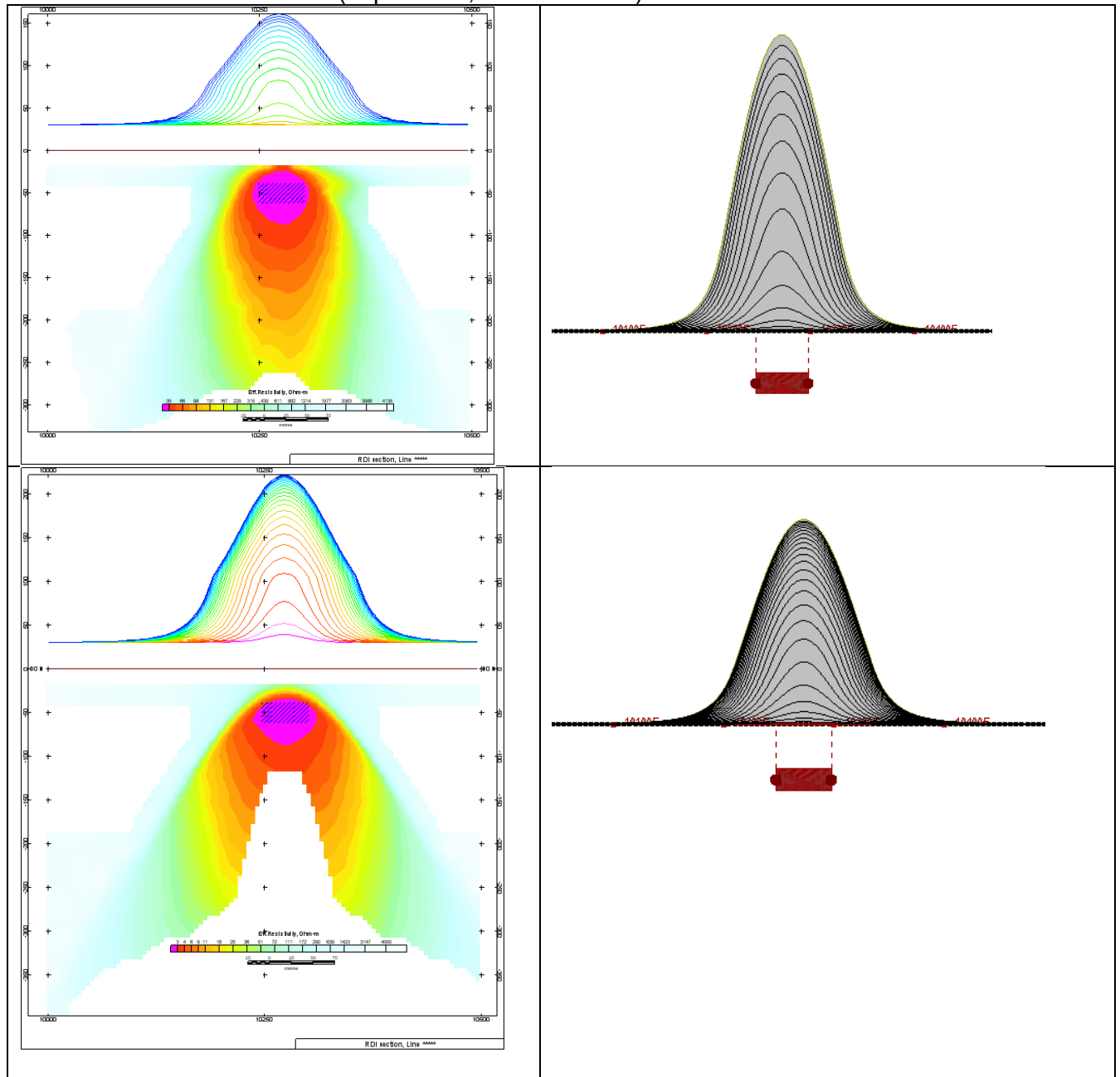


Figure F-6: Maxwell plate model and RDI from the calculated response for horizontal thick (20m) plate – less conductive (on the top), more conductive (below)

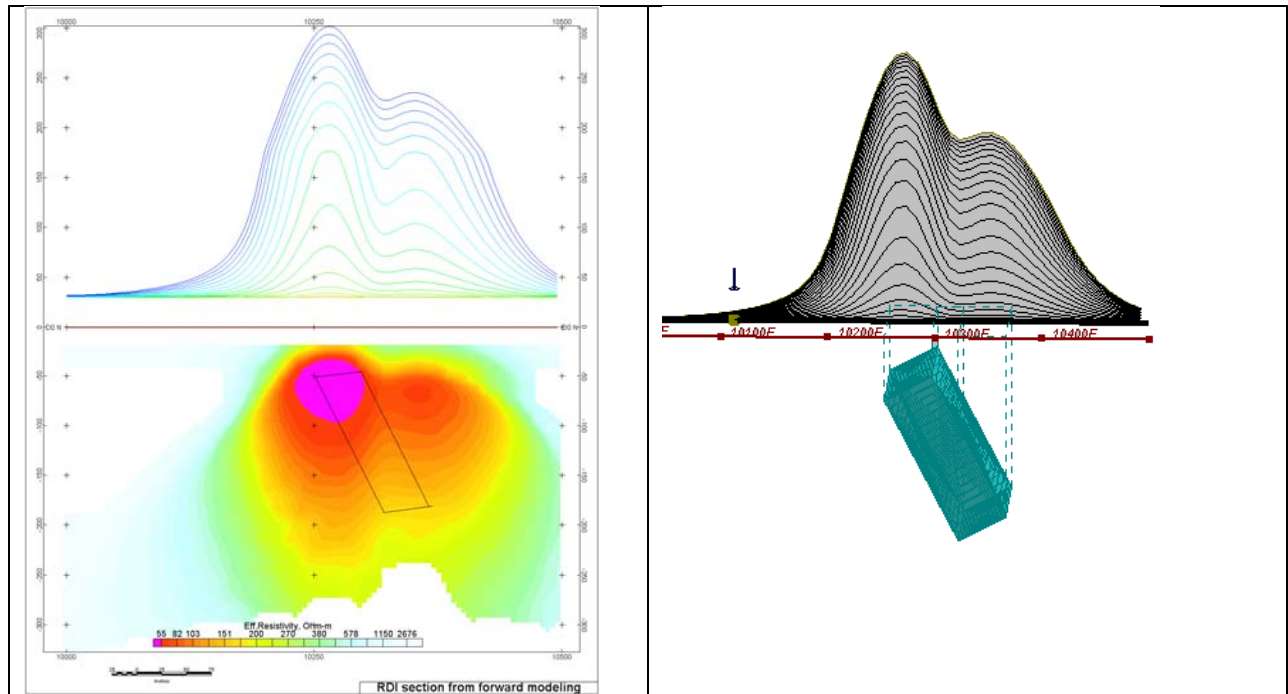


Figure F-7: Maxwell plate model and RDI from the calculated response for inclined thick (50m) plate. Depth extends 150 m, depth to the target 50 m.

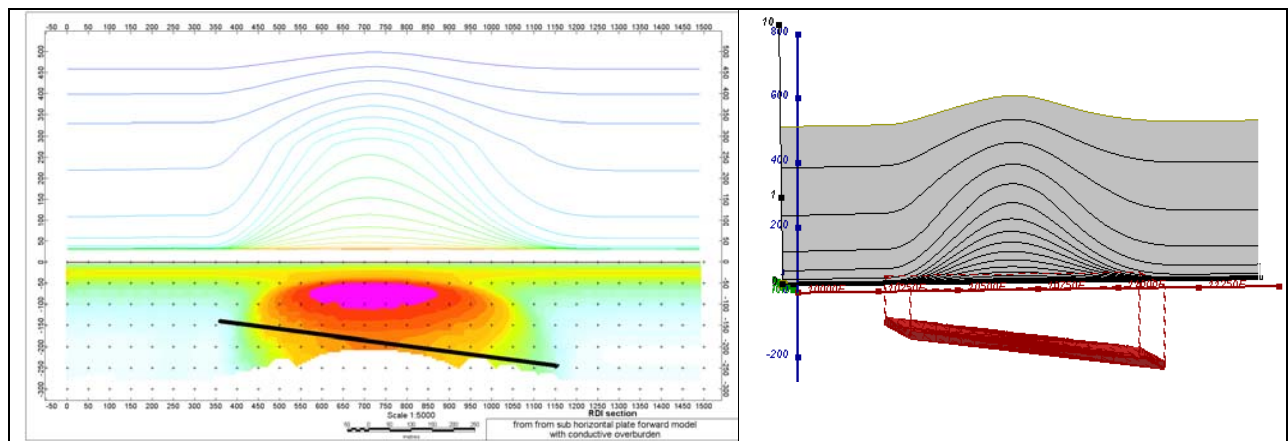


Figure F-8: Maxwell plate model and RDI from the calculated response for the long, wide, and deep subhorizontal plate (depth 140 m, dim 25x500x800 m) with conductive overburden.

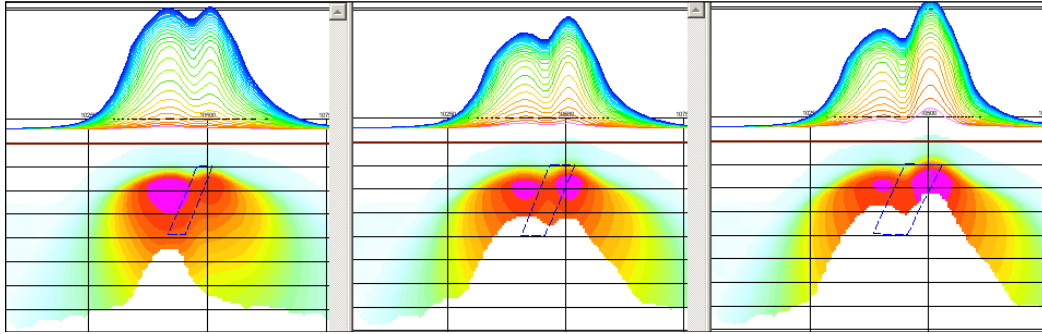


Figure F-9: Maxwell plate models and RDIs from the calculated response for “thick” dipping plates (35, 50, 75 m thickness), depth 50 m, conductivity 2.5 S/m.

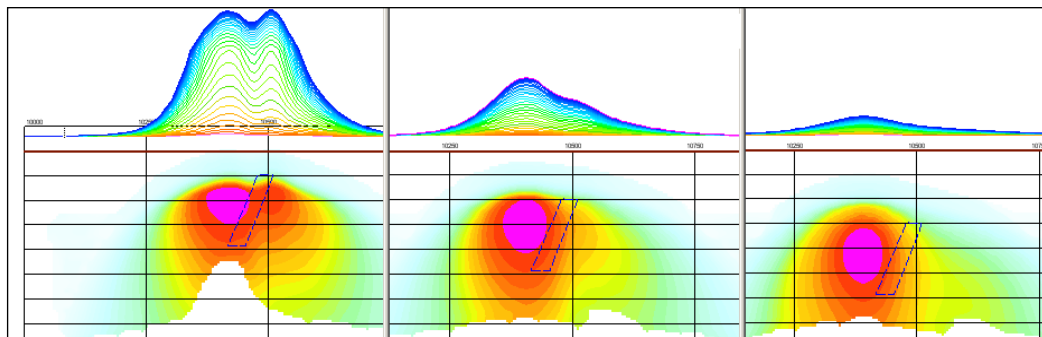


Figure F-10: Maxwell plate models and RDIs from the calculated response for “thick” (35 m thickness) dipping plate on different depth (50, 100, 150 m), conductivity 2.5 S/m.

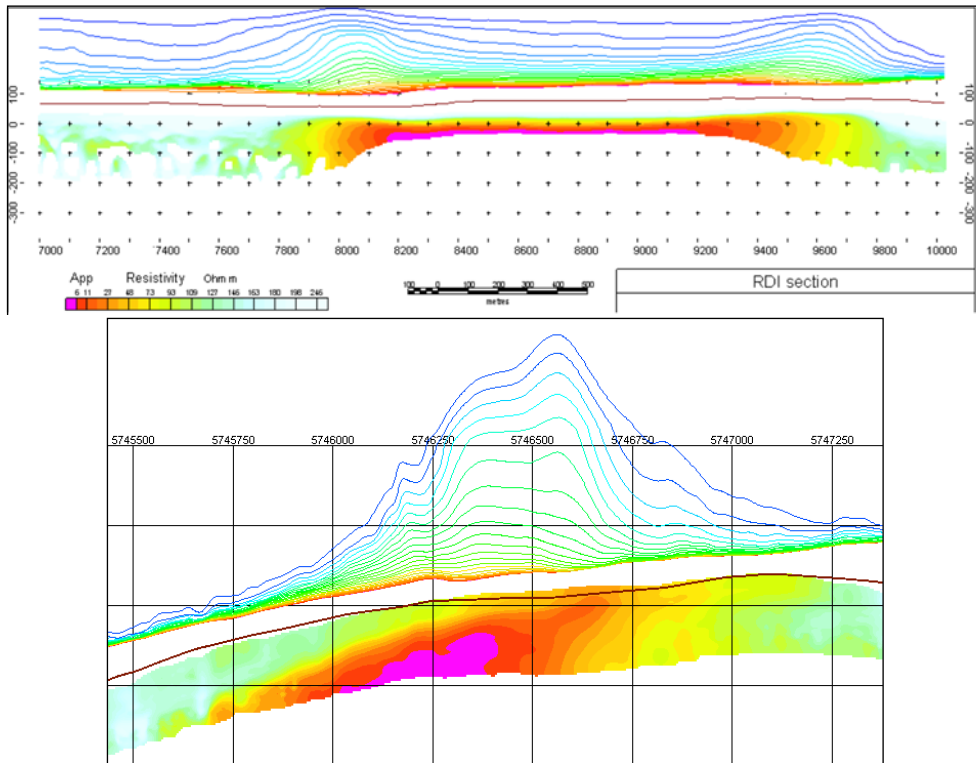
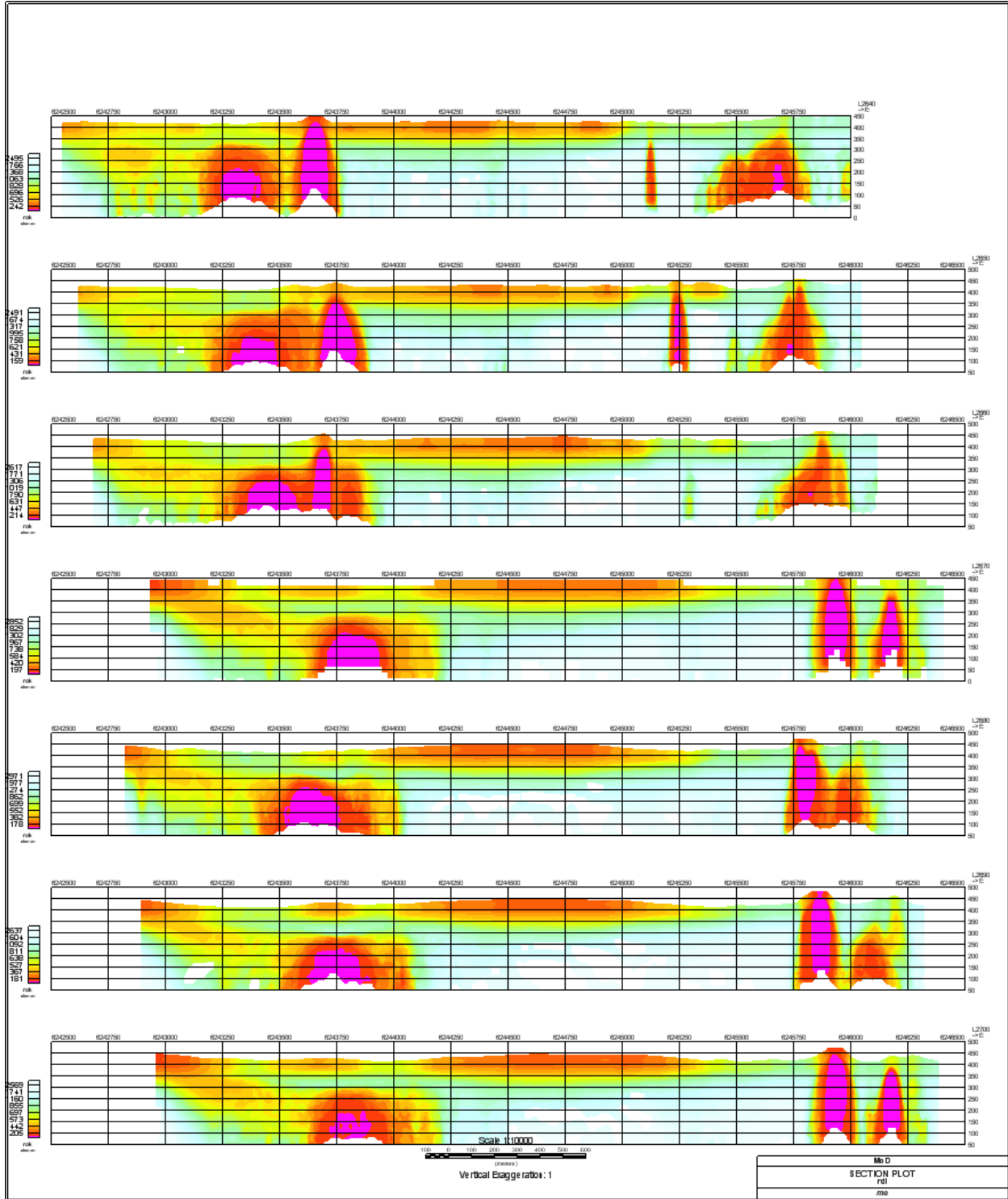


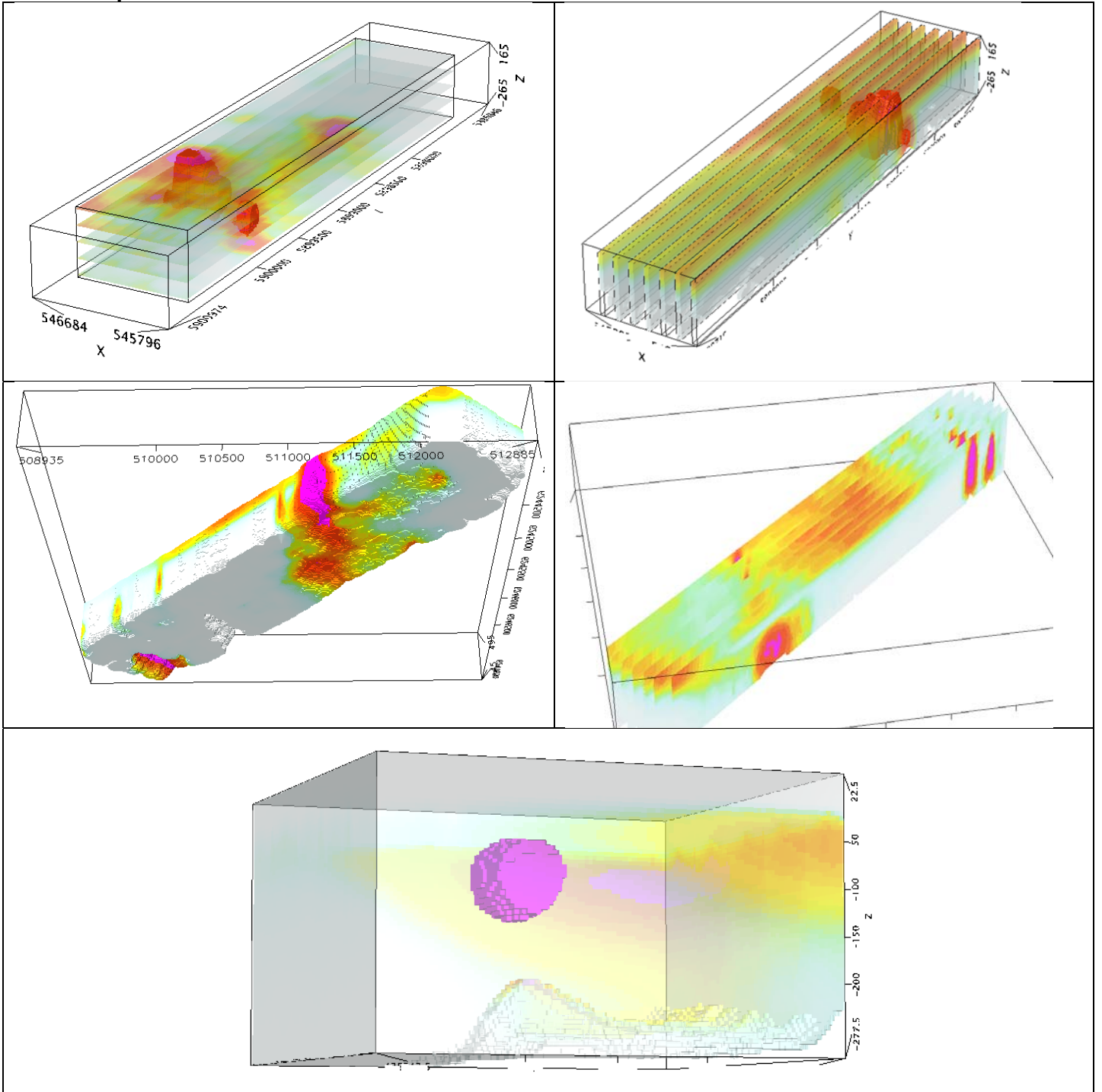
Figure F-11: RDI section for the real horizontal and slightly dipping conductive layers

FORMS OF RDI PRESENTATION

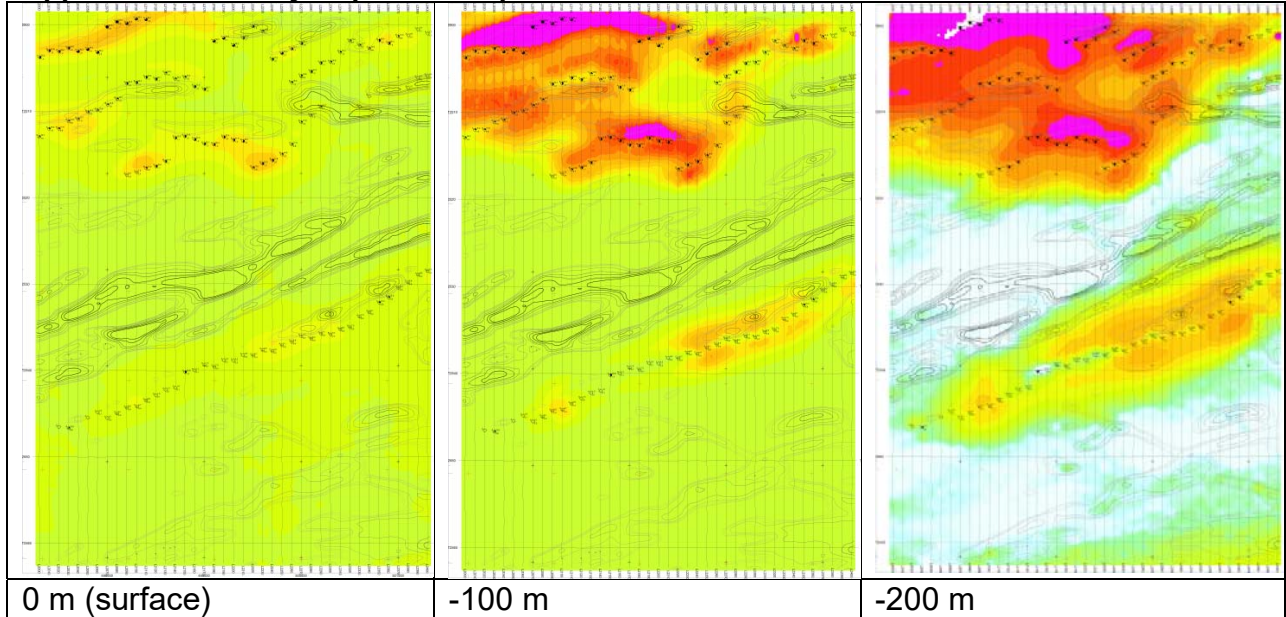
Presentation of series of lines



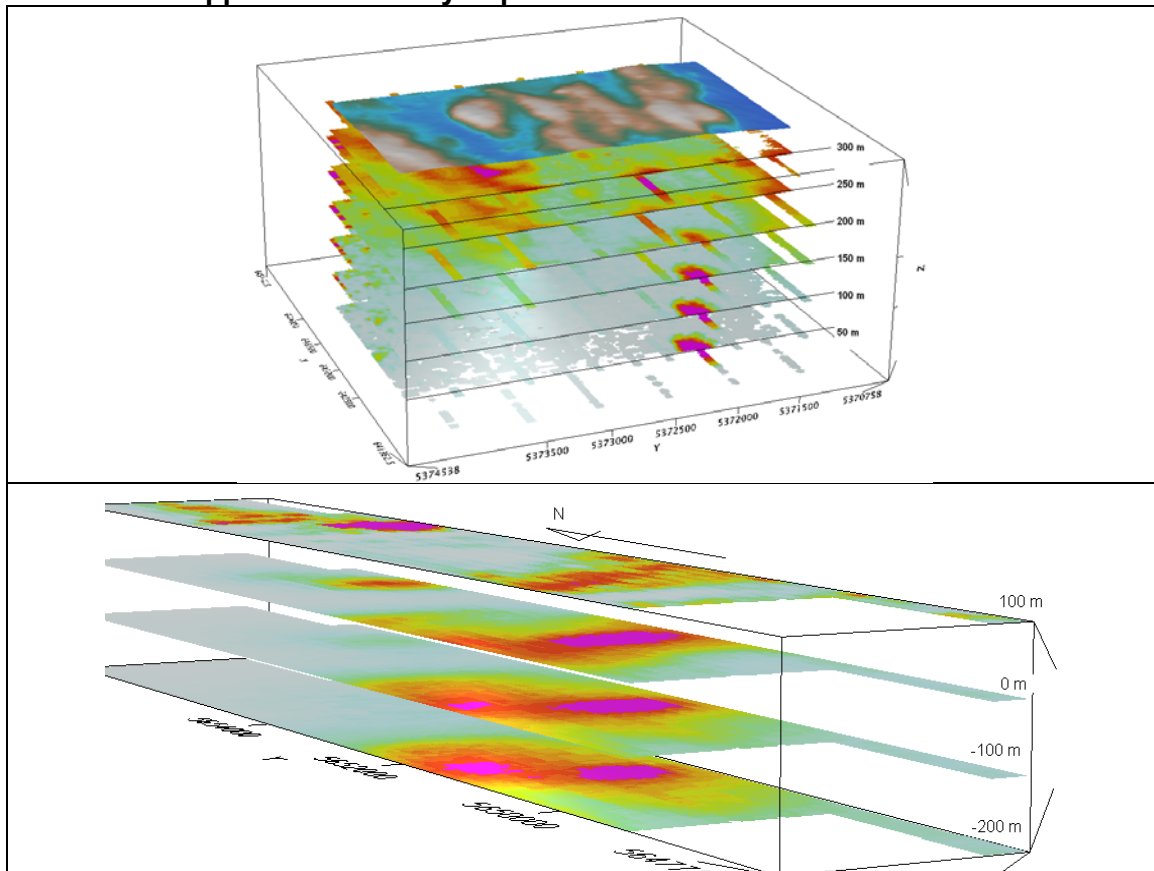
3d presentation of RDIs



Apparent Resistivity Depth Slices plans:

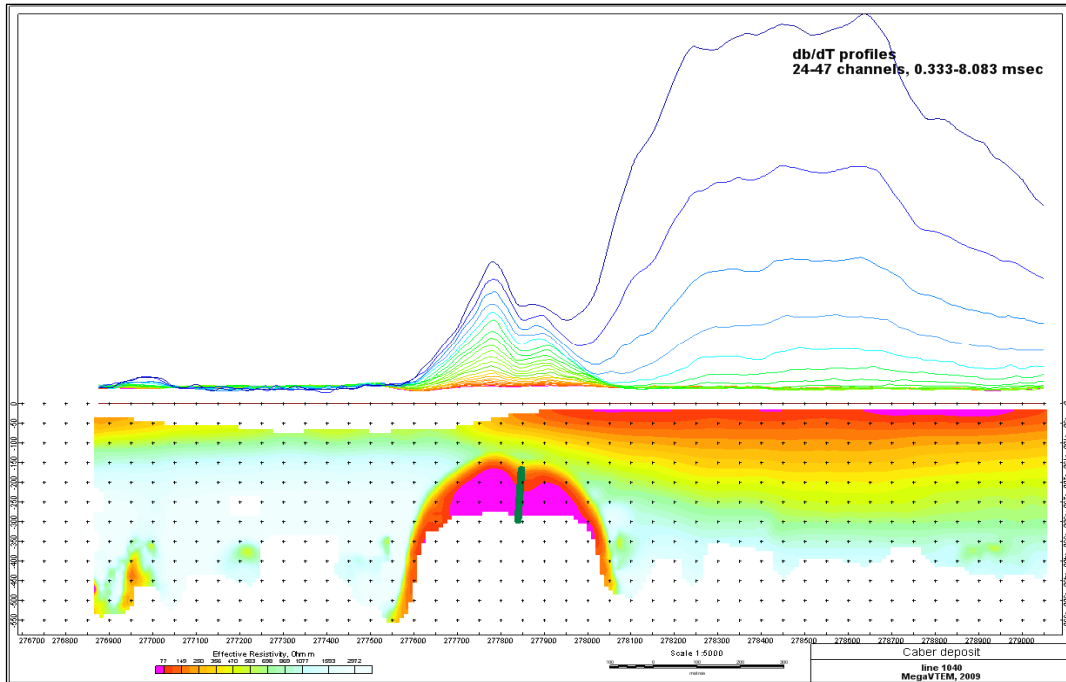


3d views of apparent resistivity depth slices:

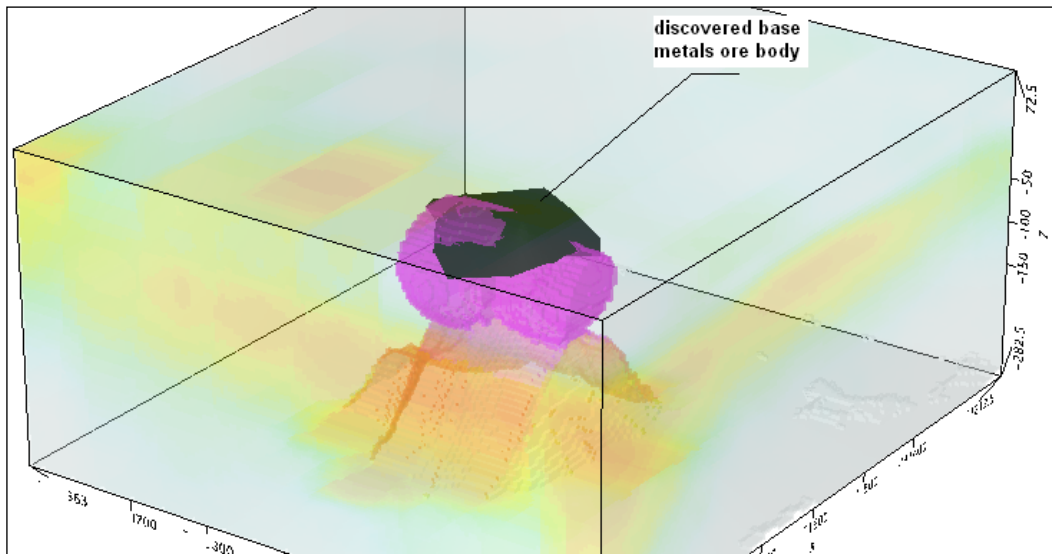


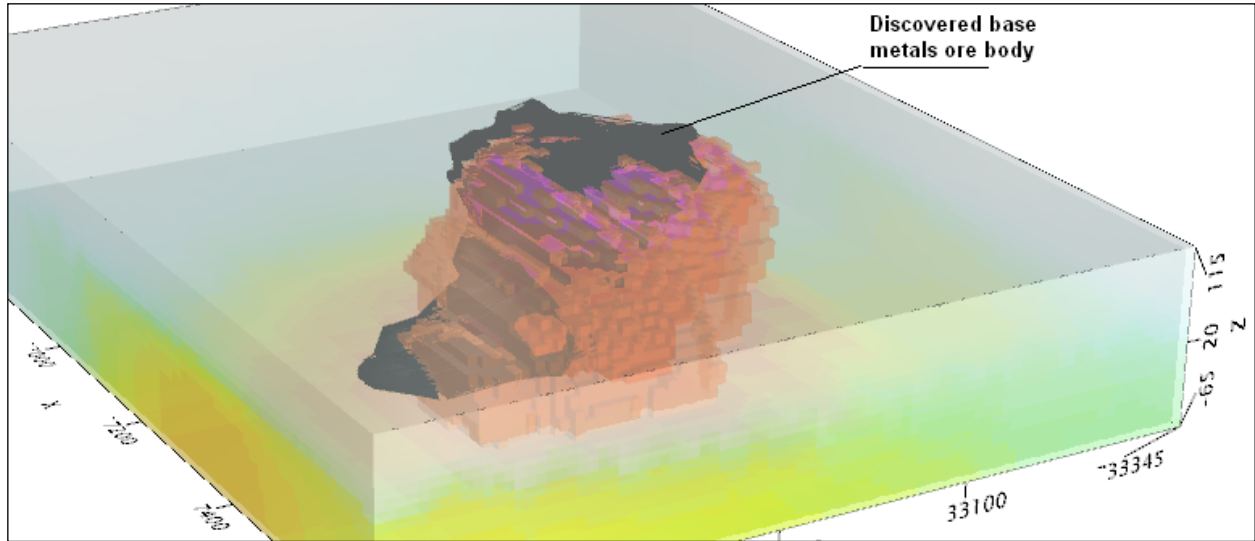
Real base metal targets in comparison with RDIs:

RDI section of the line over Caber deposit (“thin” subvertical plate target and conductive overburden).



3d RDI voxels with base metals ore bodies (Middle East):





Alexander Prikhodko, PhD, P.Geol
UTS Ltd.
April 2011

APPENDIX G
Resistivity Depth Images (RDI)
Please see attached DVD for each block RDI.